HHS Public Access

Author manuscript

Sci Transl Med. Author manuscript; available in PMC 2021 November 19.

Published in final edited form as:

Sci Transl Med. 2021 May 19; 13(594): . doi:10.1126/scitranslmed.abd1869.

ABCB10 exports mitochondrial biliverdin, driving metabolic maladaptation in obesity[$]

Michael Shum[1,2,3,13], **Chitra A. Shintre**[4], **Thorsten Althoff**[5], **Vincent Gutierrez**[1,2,3], **Mayuko Segawa**[1,2,3], **Alexandra D. Saxberg**[6], **Melissa Martinez**[6], **Roslin Adamson**[4], **Margaret R. Young**[4], **Belinda Faust**[4,14], **Raffi Gharakhanian**[1,2], **Shi Su**[7], **Karthickeyan Chella Krishnan**[8,9], **Kiana Mahdaviani**[1,7], **Michaela Veliova**[2], **Dane M. Wolf**[1,7], **Jennifer Ngo**[1,2,3,10], **Laura Nocito**[7], **Linsey Stiles**[1,2], **Jeff Abramson**[5], **Aldons J. Lusis**[3,8,11,12], **Andrea L. Hevener**[1], **Maria E. Zoghbi**[#6], **Elisabeth P. Carpenter**[#4,14], **Marc Liesa**[1,2,3,*]

[1]Department of Medicine, Division of Endocrinology, David Geffen School of Medicine at UCLA. 650 Charles E. Young Dr., Los Angeles, CA 90095 USA.

[2]Department of Molecular and Medical Pharmacology, David Geffen School of Medicine at UCLA. 650 Charles E. Young Dr., Los Angeles, CA 90095 USA.

[3]Molecular Biology Institute at UCLA, 611 Charles E. Young Dr., Los Angeles, CA 90095 USA.

[4]Center for Medicines Discovery, University of Oxford, Oxfordshire, OX3 7DQ, UK.

[5]Department of Physiology, University of California, Los Angeles, 650 Charles E. Young Dr., Los Angeles, CA 90095 USA.

[6]University of California Merced, School of Natural Sciences, 5200 North Lake Rd. Merced, CA 95343.

[7]Evans Biomedical Research Center, Boston University School of Medicine, 650 Albany st., Boston, MA 02118 USA.

[8]Department of Human Genetics, David Geffen School of Medicine at UCLA. 650 Charles E. Young Dr., Los Angeles, CA 90095 USA.

[9]Department of Pharmacology and Systems Physiology, University of Cincinnati College of Medicine, 231 Albert Sabin Way, Cincinnati, OH 45267-0575 USA.

[10]Department of Chemistry & Biochemistry, University of California, Los Angeles, CA 90095.

---

[*]Corresponding author: mliesa@mednet.ucla.edu.

Author contributions: M.L., M.Sh., C.A.S and E.P.C conceptualized the project. M.Sh., C.A.S., T.A., V.G., M.Se., M.L., R.A., M.Y., B.F., E.P.C., A.D.S., M.M., M.E.Z., T.A., J.A., A.H. and A.J.L. provided methods. M.Sh., M.L., C.A.S., T.A., V.G., M.Se., E.P.C., A.D.S., M.M., M.E.Z., R.G., K.C.K., A.H. and M.V analyzed data. M.Sh., T.A., M.L., C.A.S., V.G., M.Se., A.D.S., M.M., M.E.Z., R.G., S.S., K.M., A.H., M.V., D.M.W., J.N., L.N and L.S. performed experiments. M.L., E.P.C., M.Z., A.H., A.J.L. and J.A provided resources. M.Sh. and M.L. wrote the original draft. M.L., E.P.C and M.E.Z. supervised the project and acquired funds.

Competing interests: The following competing interests are not related to this study: E.P.C and B.F. are currently employed by Vertex Pharmaceuticals and M.L. is a co-founder and consultant of Enspire Bio LLC. The authors declare that they have no competing interests.

[11]Department of Medicine, Division of Cardiology, David Geffen School of Medicine at UCLA. 650 Charles E. Young Dr., Los Angeles, CA 90095 USA.

[12]Department of Microbiology, Immunology and Molecular Genetics, David Geffen School of Medicine at UCLA. 650 Charles E. Young Dr., Los Angeles, CA 90095 USA.

[13]Present address, Department of Molecular Medicine, Faculty of Medicine, Université Laval, Québec City, G1V 0A6, Canada

[14]Present address, Vertex Pharmaceuticals Ltd., Jubilee Drive, Milton Park, Abingdon, OX14 4RZ, UK.

[#] These authors contributed equally to this work.

Abstract

Although the role of hydrophilic antioxidants in the development of hepatic insulin resistance and non-alcoholic fatty liver disease (NAFLD) has been well studied, the role of lipophilic antioxidants remains poorly characterized. A known lipophilic H_2O_2 scavenger is bilirubin, which can be oxidized to biliverdin and then reduced back to bilirubin by cytosolic biliverdin reductase (BLVRA). Oxidation of bilirubin to biliverdin inside mitochondria must be followed by the export of biliverdin to the cytosol, where biliverdin is reduced back to bilirubin. Thus, the putative mitochondrial exporter of biliverdin is expected to be a major determinant of bilirubin regeneration and intracellular H_2O_2 scavenging. Here, we identified ABCB10 as a mitochondrial biliverdin exporter. ABCB10 reconstituted into liposomes transported biliverdin and ABCB10 deletion caused accumulation of biliverdin inside mitochondria. Obesity with insulin resistance upregulated hepatic ABCB10 expression in mice and elevated cytosolic and mitochondrial bilirubin content in an ABCB10-dependent manner. Revealing a maladaptive role of ABCB10 driven bilirubin synthesis, hepatic ABCB10 deletion protected diet-induced obese mice from steatosis and hyperglycemia, improving insulin-mediated suppression of glucose production and decreasing lipogenic SREBP-1c expression. Protection was concurrent with enhanced mitochondrial function and increased inactivation of PTP1B, a phosphatase disrupting insulin signaling and elevating SREBP-1c expression. Restoration of cellular bilirubin content in ABCB10 KO hepatocytes reversed the improvements in mitochondrial function and PTP1B inactivation, demonstrating that bilirubin was the maladaptive effector linked to ABCB10 function. Thus, we identified a fundamental transport process that amplifies intracellular bilirubin redox actions, which can exacerbate insulin resistance and steatosis in obesity.

One Sentence Summary:

ABCB10 in liver promotes hyperglycemia and steatosis.

INTRODUCTION:

H_2O_2 produced by mitochondria not only can damage cells, but it is a central molecule participating in signaling transduction as well (1). Consequently, pro- and anti-oxidant systems are key regulators of metabolism and can play tissue-specific roles. Liver is one of the tissues with the highest antioxidant capacity and largest variety of antioxidant systems. Both pro-oxidants and antioxidants are concurrently elevated in insulin resistant and

steatotic livers and are distributed to distinct microdomains based on their chemical properties. A well-studied antioxidant of the hydrophilic environment is glutathione. The lipophilic environment, which includes membranes, has its own antioxidant systems that are less studied. Among them are ubiquinol, melatonin, α-lipoic acid, and bilirubin (2). Bilirubin is a particularly interesting antioxidant due to its lipophilicity, cell-autonomous and ubiquitous production from heme degradation and its presence in different organelles (3, 4).

Heme is an essential cofactor present in all cell types, as it is part of mitochondrial cytochromes and oxygen carrier proteins. However, free heme is toxic, as it can cause oxidative damage (5). Consequently, all cells prevent heme-induced toxicity by degrading heme to biliverdin. Biliverdin is soluble and is transformed by cytosolic biliverdin reductase (BLVRA) to lipophilic bilirubin (6, 7). Bilirubin and biliverdin are both released from the cytosol to the bloodstream. Plasma bilirubin concentrations are higher (1–25 μM) than biliverdin (0.12–0.01 μM), which is explained by the efficient and ubiquitous conversion of biliverdin to bilirubin and the faster excretion of biliverdin. Indeed, biliverdin can be directly excreted to the bile (8), whereas solubilization of bilirubin is required for its efficient excretion. Bilirubin solubilization is achieved by conjugating bilirubin to glucuronic acids, a reaction catalyzed by UGT1A1 in the endoplasmic reticulum (ER) lumen of hepatocytes (9).

The lipophilicity of unconjugated bilirubin allows its passive diffusion through cellular membranes, including mitochondrial membranes (10). Kernicterus, a neurological disease resulting from excessive plasma bilirubin concentrations (>300μM), damages brain mitochondria (11). The detrimental effect of high bilirubin concentrations on mitochondrial function can be reproduced *in vitro*, as 100 μM bilirubin added to isolated mitochondria completely blocks their ATP synthesis capacity (12). In contrast, 100 μM biliverdin has no effects on isolated mitochondrial function (12). Moreover, bilirubin decreases mitochondrial OXPHOS efficiency (12), scavenges lipid peroxides and decreases H_2O_2 content at low micromolar, even nanomolar concentrations (6, 7).

Consequently, the intracellular pool of free bilirubin must be tightly regulated to prevent the toxic actions of bilirubin on mitochondria and execute its beneficial actions when needed. The lipophilic nature of bilirubin and higher hydrophilicity of biliverdin impose a mechanistic challenge on the regulation of their intracellular pools. Bilirubin can cross membranes by passive diffusion and equilibrate across the ER, mitochondria, and cytosol (10). When bilirubin scavenges H_2O_2, it is oxidized to form biliverdin, which cannot cross membranes easily. Indeed, there is functional evidence that an uncharacterized biliverdin exporter is present in the plasma membrane of hepatocytes and is required to export biliverdin to the bile (8). However, whether mitochondria export biliverdin is unknown. Biliverdin cannot be converted back to bilirubin in the mitochondrial matrix, as BLVRA is absent (13, 14). Therefore, mitochondria can regulate bilirubin synthesis by controlling the export of biliverdin. The regulation of mitochondrial biliverdin export and its consequences on the cellular pool of bilirubin, as well as on mitochondrial bilirubin content, are currently undefined.

The ATP binding cassette (ABC) transporter ABCB10 is located in the inner mitochondrial membrane (15–18) and is highly expressed in the liver and bone marrow. ABCB10 is

essential for hemoglobinization during primitive erythropoiesis and ABCB10 deletion causes defects in hemoglobin synthesis that are rescued by treatments with antioxidants. This rescue by antioxidants demonstrates that ABCB10 is not essential for heme synthesis *per se,* but rather protects from oxidative stress induced by high heme content (16). Hepatocytes are ranked second after differentiating erythrocytes as the cells with the highest rates of heme synthesis in their mitochondria (19). Disturbed heme homeostasis and changes in mitochondrial function in liver are associated with insulin resistance and fatty liver disease (20), and *ABCB10* is the only gene that encodes for a mitochondrial transporter related to heme homeostasis with intronic variants associated with type 2 diabetes (21, 22). However, the function of ABCB10 in liver, its role in insulin resistance, and the cargo transported by ABCB10 are unknown.

Here, we demonstrate that ABCB10 is a mitochondrial biliverdin exporter that increases bilirubin production. We find that ABCB10 upregulation is necessary for the increase in mitochondrial bilirubin content induced by obesity, which leads to a redox state that promotes hepatic steatosis and insulin resistance. In all, we define a mitochondrial transport process that becomes maladaptive in obesity.

RESULTS

ABCB10 exports biliverdin, which increases bilirubin synthesis

ABCB10 has been mostly studied in differentiating red blood cells (15–18, 23). As the substrate exported by ABCB10 is unknown, the mechanism by which ABCB10 protected from oxidative damage is uncharacterized (16). However, previous data provided key insights about the nature of ABCB10 cargo. Treating ABCB10 knockout (KO) red blood cell precursors with antioxidants rescues heme biosynthesis, showing that ABCB10 is not essential to transport heme intermediates and heme itself (16, 24). Instead, the cargo transported by ABCB10 is expected to counteract oxidative stress and to be produced during heme synthesis.

In this context, the next logical molecules to test as ABCB10 cargo were the products of heme metabolism, biliverdin and its redox pair bilirubin (fig. S1A). ABC transporters harness energy from the hydrolysis of ATP to facilitate the conformational changes necessary to execute transport cycles. Thus, ABCB10 ATPase activity is expected to increase in the presence of its cargo (24, 25). We found that biliverdin, but not bilirubin, caused a 2-fold increase in ABCB10 ATPase activity in purified human ABCB10 reconstituted into nanodiscs (Fig. 1A). Maximal ATPase activation was achieved at biliverdin concentrations of 2.5–5 μM with a Km of 143.6 nmols biliverdin/mg protein/min and a Vmax of 323 nmols Pi/mg protein/min (Fig. 1B). Moreover, other heme-related molecules previously hypothesized to be transported by ABCB10, including heme precursors aminolevulinic acid (ALA) and protoporphyrin IX, as well as hemin, did not change ABCB10 ATPase activity (26, 27). Altogether, these results support that biliverdin is the only heme-related candidate as cargo transported by ABCB10.

To directly determine whether ABCB10 transports biliverdin across membranes, we reconstituted human ABCB10 into sealed liposomes. For ABC transporters that carry a

substrate away from the ATP domain, cargo accumulation inside liposomes can be achieved by adding ATP in the incubation media. The reason is that ATP cannot cross the membrane of a sealed liposome and thus ATP is not accessible to transporters inserted in the opposite orientation. As a result, ABCB10 molecules with their ATP binding domain facing the incubation media will be the only ABCB10 molecules transporting cargos, allowing the cargo to accumulate inside liposomes (Fig. 1C).

With ATP in the media, we observed a linear increase in radioactive biliverdin accumulation in ABCB10-liposomes, approaching a plateau 15–30 minutes after adding radioactive biliverdin (Fig. 1D). In the absence of ATP, we detected a minor and linear increase in radioactive biliverdin content in liposomes. We attributed the ATP-independent increase in biliverdin accumulation to the expected binding of biliverdin to lipids and maybe to ABCB10 itself, but without being transported. This ATP-independent increase in biliverdin accumulation was subtracted to calculate the maximal amount of biliverdin transported by ABCB10. After 60 minutes of incubation, 135 nmols of biliverdin/mg ABCB10 protein accumulated into the liposomes (Fig. 1D). To further confirm the specificity of ABCB10-mediated biliverdin transport, we tested the ability of the heme-related molecules, as well as unlabeled biliverdin, to compete for ABCB10-mediated labeled biliverdin uptake. As expected, un-labelled biliverdin (1 μM, 3-fold higher than labelled) blocked labelled biliverdin uptake, whereas the other physiological heme-related molecules did not (fig. S2). In all, these data support that the only heme-related molecule transported by ABCB10 is biliverdin.

As bilirubin is synthesized in the cytosol from biliverdin by BLVRA, our expectation was that ABCB10-mediated biliverdin export would increase cytosolic bilirubin production and availability (fig. S3). If this expectation was correct, ABCB10 gain-of-function would increase bilirubin content in the cytosol of hepatocytes. Then, higher cytosolic bilirubin availability would lead to an increase in mitochondrial bilirubin through passive diffusion across mitochondrial membranes (10). The availability of a fluorescent and reversible bilirubin sensor, the eel protein UnaG (4, 28) (Fig. 1E), allowed us to perform real-time measurements of cytosolic and mitochondrial bilirubin in live cells. UnaG was successfully targeted to the mitochondrial matrix of mouse primary hepatocytes, as shown by its co-localization with TMRE (Fig. 1E). UnaG fluorescence successfully reported mitochondrial bilirubin content, as shown by the increase in UnaG fluorescence after adding bilirubin to the media (fig. S4A–B) (3, 4). Increasing ABCB10 expression in AML12 murine hepatocytes elevated both cytosolic and mitochondrial bilirubin content (Fig. 1F and fig. S5), supporting that ABCB10-mediated biliverdin export was sufficient to increase bilirubin synthesis.

Hepatic ABCB10 expression is higher in diet-induced obese mice and is associated with greater steatosis and insulin resistance

As insulin resistance induces hepatic redox stress and intronic *ABCB10* variants are associated with type 2 diabetes in humans (21, 22), we analyzed hepatic *Abcb10* expression in the Western diet-fed Hybrid Mouse Diversity Panel (HMDP). The HMDP is a collection of 102 mouse strains with obesity, insulin resistance, and hepatic steatosis (29). *Abcb10*

mRNA content in liver is elevated by Western diet feeding in 68 of the 102 HMDP strains, with 68 being the number of strains with matched chow diet feeding. The increase in ABCB10 expression ranged 2–10-fold depending on the strain (Fig. 1G). Analyzing the 102 Western diet fed HMDP strains, we found a positive correlation between hepatic *Abcb10* expression and the severity of steatosis and insulin resistance (Fig. 1H and fig. S6A,B). Accordingly, liver *Abcb10* expression showed positive and significant correlations with liver triglyceride content ($p=0.0033$), HOMA-IR values ($p=0.0057$), and fasting insulin concentrations ($p=0.0008$) (Fig. 1H and fig. S6A–C). Correlations were determined via midweight bicorrelation analyses as reported (29). No significant ($p>0.05$) correlations of liver *Abcb10* expression with gonadal fat mass were detected (Fig. 1I and fig. S6D). Thus, hepatic ABCB10 upregulation was not a reflection of the different susceptibility among HMDP strains to develop obesity. Last, ABCB10 protein was also increased in liver from C57BL/6J mice fed a 45% high-fat diet (Fig. 1J).

ABCB10 is dispensable for normal hepatocyte function in mice

Liver is ranked second in the list of tissues with the highest ABCB10 content and heme synthesis rates (30). To determine the physiological relevance of ABCB10-mediated biliverdin export in hepatocytes, we first tested the effects of deleting ABCB10 in hepatocytes from control lean mice by generating *Abcb10* liver-specific KO mice (LKO) (fig. S7). *Abcb10* excision was confirmed by amplification of the Cre-excised *Abcb10* genomic sequence and elimination of ABCB10 protein from primary hepatocytes isolated from LKO mice (Fig. 2A,B). Phenotypically, LKO mice were healthy with normal body weight, glucose tolerance, hepatic lipid content, and mitochondrial function (Fig. 2C–G). In marked contrast to erythroid cells (16), ABCB10 is not essential for viability, mitochondrial function, or heme homeostasis in hepatocytes. If ABCB10 exported biliverdin in hepatocytes *in vivo*, biliverdin would accumulate in ABCB10 KO mitochondria. Relative quantifications of mitochondrial biliverdin content revealed a 79% increase in isolated mitochondria from LKO mice, showing that the absence of ABCB10 caused accumulation of biliverdin in mitochondria (Fig. 2H). As expected from a decrease in bilirubin synthesis induced by an abrogation of ABCB10-mediated biliverdin export, ABCB10 deletion decreased both cytosolic and mitochondrial bilirubin content in primary hepatocytes (Fig. 2I,J). These data indicate that mitochondrial biliverdin export by ABCB10 contributes to bilirubin production in mouse hepatocytes, and that neither ABCB10 deletion nor elevated mitochondrial biliverdin are deleterious for normal liver function in mice.

Hepatic ABCB10 deletion protects diet-induced obese mice from insulin resistance

The positive correlation between hepatic ABCB10 expression and insulin resistance suggested two possible roles for ABCB10: either ABCB10 exacerbates insulin resistance or ABCB10 ineffectively counteracts insulin resistance. Supporting the first role, ABCB10 liver-specific KO (LKO) mice were protected from glucose intolerance induced by high-fat diet (HFD) and showed improved glucose clearance during a GTT without changes in insulinemia (Fig. 3A–B), as well as a prolonged action of insulin maintaining lower glycemia during an ITT (Fig. 3C). ABCB10 deletion decreased fasting glucose concentrations, without changing fasting insulin (Fig. 3D–E). A 7.2% decrease in body

weight without changes in food intake was observed in HFD-fed LKO mice, which was explained by lower fat mass (Fig. 3F–H).

The improvement in the glycemic profiles of LKO mice could be a result of a decrease in hepatic glucose production and an improvement in insulin action suppressing hepatic glucose production. Consequently, to test whether changes in hepatic glucose production in LKO mice were independent of decreased body weight, we used weight-matched HFD-fed LKO and WT mice (Fig. 3I) to perform hyperinsulinemic-.euglycemic clamps (Fig. 3J). These clamp experiments revealed that glucose infusion rates in weight-matched HFD-fed LKO mice were 48% higher than in WT littermates (Fig. 3K). Hepatic glucose production was markedly decreased and the ability of insulin to suppress hepatic glucose production was improved in HFD-fed LKO mice (Fig. 3L–M). Higher suppression of hepatic glucose production by insulin, without a change in insulin-stimulated glucose disappearance rates (Fig. 3N), indicated that protection from insulin resistance in LKO mice was largely restricted to the liver. Thus, these data support that ABCB10 deletion in liver might not protect muscle from insulin resistance.

ABCB10 impairs insulin signaling in primary human and mouse hepatocytes

Although hepatic glucose production rates can be determined by extrahepatic tissues, impaired insulin signal transduction in liver can augment hepatic glucose production and is a reliable biomarker of hepatocyte-autonomous insulin resistance (31–33). To determine whether ABCB10 deletion improved insulin sensitivity in a hepatocyte-autonomous manner, we isolated primary hepatocytes from weight-matched HFD-fed WT and ABCB10 LKO mice and determined insulin action *ex vivo*. To this end, we measured the effects of insulin treatment on the insulin receptor (INSR) and AKT phosphorylation in cultured primary hepatocytes. After five minutes treatment of 10 nM insulin, HFD-fed LKO primary hepatocytes showed a 2-fold improvement in the action of insulin increasing INSR Tyr1162/1163 and AKT Ser473 phosphorylation, when compared to hepatocytes from HFD-fed WT littermates (Fig. 4A). In healthy primary human hepatocytes with ABCB10 knocked down (40%) (fig. S8A), a similar improvement in insulin action on INSR Tyr1162/1163 phosphorylation was observed (Fig. 4B).

To test whether elevated ABCB10 function was sufficient to decrease insulin signaling in human hepatocytes, we used adenoviral transduction to increase ABCB10 expression (fig. S8B). The ability of insulin (10 nM) to induce INSR and AKT phosphorylation was decreased both in mouse AML12 and primary human hepatocytes with increased ABCB10 expression (Fig. 4C,D). Last, we restored ABCB10 expression *ex vivo* via adenoviral transduction of primary hepatocytes isolated from HFD-fed ABCB10 LKO mice. We found that the improvement in insulin action phosphorylating INSR and AKT in LKO hepatocytes was reversed by ABCB10 re-expression (fig. S9).

Our data show that high ABCB10 expression promotes a hepatocyte-autonomous disruption in insulin signaling in mouse and human hepatocytes. Accordingly, ABCB10 deletion in HFD-fed mice improved insulin signaling, decreased hepatic glucose production, and increased the action of insulin suppressing hepatic glucose production in HFD-fed mice.

Hepatic ABCB10 deletion increases mitochondrial respiration, protects from steatosis, and counteracts hyperlipidemia in diet-induced obese mice

To investigate why HFD-fed ABCB10 LKO mice showed decreased fat mass, we measured their energy balance using CLAMS. No significant changes ($p > 0.05$) were detected in their food intake, fecal lipids (Fig. 5A, B), or total physical activity (fig. S10A). In contrast, we detected a significant ($p < 0.05$) increase in oxygen consumption (VO_2) and energy expenditure (EE) in HFD-fed LKO mice at night (fed state) when using co-variate statistics to model VO_2 and EE values at an equal body weight between genotypes (Fig. 5C, D). HFD-fed LKO mice showed an elevation in carbohydrate oxidation, revealed by higher respiratory exchange rates (RER) at night (Fig. 5E). Thus, increased RER showed that the decrease in body fat in LKO mice was associated with increased carbohydrate expenditure, rather than elevated fat expenditure. Accordingly, we did not observe changes in circulating FGF21 in ABCB10 LKO mice (fig. S10B), a factor secreted by the liver that increases systemic energy expenditure by promoting fat oxidation (34).

Higher mitochondrial oxidative function in hepatocytes was previously shown to improve insulin signaling (20, 35). To test whether ABCB10 deletion increased mitochondrial function in diet-induced obese mice, we isolated mitochondria and primary hepatocytes from livers of HFD-fed ABCB10 LKO mice and measured their respiratory capacity. Respiration coupled to ATP synthesis was increased both in isolated mitochondria and in primary hepatocytes isolated from HFD-fed ABCB10 LKO mice (Fig. 5F, G). Maximal respiratory capacity was increased in primary hepatocytes from HFD-fed LKO mice as well (Fig. 5H). These changes in mitochondrial function occurred in the absence of changes in mitochondrial biogenesis markers, such as PGC-1α (PPARγ coactivator-1 alpha) or TFAM (Transcription factor A, mitochondrial) (fig. S10C), and without a coordinated upregulation in the subunits of mitochondrial complexes I, III, IV and V (Fig. 5I, J). Altogether, our data showed that ATP-synthesizing capacity (OXPHOS) was improved per unit of mitochondria with ABCB10 deleted. In this regard, we observed a 50% upregulation exclusively in complex II content (Fig. 5I, J). The specific upregulation of complex II in ABCB10 KO mitochondria suggests that bilirubin might not just be decreasing electron transfer activity as previously reported (12), but might decrease the total content of complex II as well. These data support that the regulation of complex II content could be an additional mechanism by which bilirubin is decreasing mitochondrial function and ROS production.

As hepatic steatosis is associated with insulin resistance and metabolic dysfunction, we measured lipid content and lipogenic gene expression in livers from HFD-fed LKO mice. Liver histology revealed decreased lipid droplet area in livers from HFD-fed LKO mice (Fig. 5K), which was confirmed by the 40% reduction in total triglyceride (TG) content (Fig. 5L). Moreover, HFD-fed LKO mice showed a significant ($p<0.05$) reduction in plasma TG and VLDL concentrations and a non-significant ($p>0.05$) decrease in plasma cholesterol content (Fig. 5M–O). Last, HFD-fed LKO mice showed a 50% decrease in the mRNA content of the master regulator of lipogenesis *Srebp1c* and its downstream target, fatty acid synthase (*Fasn*) (Fig. 5P). Altogether, these data support that decreased hepatic triglyceride synthesis can contribute to protection from steatosis and hyperlipidemia in LKO mice.

ABCB10 expression induced by high-fat diet hinders cytosolic and mitochondrial H_2O_2-redox signaling by elevating cellular bilirubin content

Our data show that ABCB10 gain of function was sufficient to increase mitochondrial bilirubin content in hepatocytes. However, the effects on obesity and insulin resistance on mitochondrial bilirubin content have not been measured. Consistent with the increase in ABCB10 expression induced by high-fat diet (HFD), HFD feeding elevated both mitochondrial and cytosolic bilirubin content by 50%in isolated primary hepatocytes, and these HFD-induced increases were completely prevented by ABCB10 deletion (Fig. 6A, B). In addition, we validated that the total content of the bilirubin sensor UnaG was not altered by ABCB10 deletion (fig. S11), as expected given that UnaG was delivered via viral transduction. Furthermore, ABCB10 deletion did not change the content of proteins involved in heme catabolism (HMOX1), bilirubin synthesis (BLVRA) (fig. S12), or excretion (ABCC2) (fig. S13A). Moreover, the expression of the main enzyme involved in free bilirubin conjugation, UGT1A1, was not changed by ABCB10 deletion (fig. S13B). UGT activity, mostly determined by UGT1A1, showed a non-significant ($p>0.05$) decrease in ABCB10 KO livers, which could be reflecting an unsuccessful compensation trying to preserve free bilirubin content (fig. S13C). Altogether, these data support that a major driver of increased intrahepatic bilirubin content induced by HFD was bilirubin synthesis from mitochondrial biliverdin exported by ABCB10.

A major action of bilirubin is to decrease H_2O_2 content as well as mitochondrial OXPHOS, a source of H_2O_2. H_2O_2 released by mitochondria generates signals that improve insulin signaling and prevent hepatic steatosis (20, 36). Thus, as expected from decreased bilirubin content in ABCB10 KO hepatocytes, we explored whether ABCB10 deletion caused an increase in mitochondrial H_2O_2 release and H_2O_2-mediated actions regulating the activity of redox-sensitive proteins. Using ratiometric roGFP2 probes, we measured H_2O_2 and its action on the glutathione redox state (GSSG/GSH) in live primary murine hepatocytes. Concurrently with higher mitochondrial and cytosolic H_2O_2 content (Fig. 6C–D), both mitochondrial and cytosolic GSSG/GSH were increased in live hepatocytes isolated from HFD-fed LKO mice (Fig. 6E–F). The magnitude of the elevation in H_2O_2 content and in the GSSG/GSH ratio (ranging 25–40%), together with improved mitochondrial respiration, show that the increase in H_2O_2 induced by hepatic ABCB10 deletion was not in the toxic range.

Protein Tyrosine Phosphatase 1B is increased by HFD-feeding and plays a dual maladaptive action: PTP1B directly dephosphorylates Tyr1162/1163 in INSR, blocking insulin signaling, and activates a different signaling cascade that increases *Srebp1c* expression (37–39). Furthermore, PTP1B oxidative inactivation is one of the mechanisms by which mitochondrial H_2O_2 release was demonstrated to protect from insulin resistance and hepatic steatosis (20). Consequently, we determined the effects of ABCB10 deletion in HFD fed mice on PTP1B activity. By immunoprecipitating endogenous PTP1B from total lysates of primary hepatocytes, we found that HFD-fed ABCB10 LKO mice showed a ~30% decrease in PTP1B phosphatase activity (Fig. 6G).

In sum, ABCB10 driven increases in cellular bilirubin content generate a redox state favoring insulin resistance and steatosis, by disrupting mitochondrial H_2O_2 actions on

insulin signaling (fig. S14). To determine the causal role of bilirubin in these redox changes, we next aimed to restore bilirubin content in ABCB10 KO hepatocytes and test its effects on redox and PTP1B activity (Fig. 7A).

Bilirubin supplementation reverses the redox benefits induced by ABCB10 deletion in diet-induced obese mice

Supplementing primary hepatocytes isolated from HFD-fed LKO mice with physiological bilirubin concentrations (10 μM) effectively restored mitochondrial and cytosolic bilirubin to WT concentrations (Fig. 7A and fig. S4C). Moreover, the slope of the fold increase in UnaG fluorescence over time after adding bilirubin was the same in WT and LKO hepatocytes (fig. S4A,B), supporting that the capacity of extracellular bilirubin to reach both the cytosol and the mitochondrial matrix was not changed by ABCB10 deletion. One could hypothesize that the lower content of bilirubin in LKO could accelerate the entry of bilirubin into hepatocytes. However, our data showing the absence of an acceleration suggests that the occupancy of bilirubin acceptor(s) by other competing molecules could be increased by ABCB10 deletion, or that intracellular bilirubin content is not a parameter strongly determining bilirubin entry rates.

We next tested the relationship between decreased bilirubin and the redox changes induced by ABCB10 deletion. Restoring bilirubin in HFD-fed LKO hepatocytes brought mitochondrial H_2O_2 content and GSSG/GSH back to HFD-fed WT values (Fig. 7B, C). In WT hepatocytes, HFD-feeding significantly ($p<0.05$) increased only cytosolic H_2O_2 content and, accordingly, bilirubin supplementation significantly ($p<0.05$) decreased only cytosolic H_2O_2 in HFD-fed WT hepatocytes (Figs. 6C, 7B).

As ABCB10 deletion increased mitochondrial OXPHOS, which can elevate H_2O_2 release, we tested whether restoring bilirubin content could reverse the positive effects on mitochondrial respiration observed in ABCB10 KO hepatocytes. Bilirubin 10 μM reversed the increase in mitochondrial OXPHOS observed in primary hepatocytes from HFD-fed ABCB10 LKO mice without changing OXPHOS in WT hepatocytes (Fig. 7D–E). The acute nature of bilirubin actions on mitochondria was further supported by the reversal of increased respiration when bilirubin was added to liver mitochondria isolated from HFD-fed LKO mice (Fig. 7F).

We determined whether bilirubin-mediated reversal of ABCB10 KO actions on mitochondrial redox impacted PTP1B activity. Bilirubin induced a non-significant ($p > 0.05$) increase in PTP1B activity in WT hepatocytes from HFD mice (Fig. 7G), consistent with bilirubin decreasing cytosolic H_2O_2 content (Fig. 7B) and thus PTP1B oxidative inactivation (40). Last, the same bilirubin treatments completely reversed the reduction of PTP1B activity observed in ABCB10 KO hepatocytes isolated from HFD-fed mice (Fig. 7G). Altogether, these results show that bilirubin is the major effector of ABCB10-mediated redox actions in hepatocytes from HFD-fed mice (fig. S15).

DISCUSSION

We have identified that ABCB10 exports biliverdin out of the mitochondria to amplify bilirubin synthesis. Our cell-free approach using human ABCB10 reconstituted in vesicles demonstrates that ABCB10 transports biliverdin from the matrix to the intermembrane space (IMS) domain of ABCB10. Mitochondrial biliverdin export was confirmed *in vivo* by the accumulation of biliverdin in ABCB10 KO mitochondria isolated from mouse liver. Up to this study, it was known that ABCB10 supported hemoglobin synthesis in differentiating erythrocytes, by preventing oxidative damage associated with heme synthesis (16, 30). Thus, how does biliverdin export then protect from oxidative damage?

We find that mitochondrial biliverdin export executed by ABCB10 increases the availability of biliverdin destined for bilirubin synthesis, as the enzyme transforming biliverdin to bilirubin is located in the cytosol (BLVRA). Bilirubin is an effective antioxidant that scavenges H_2O_2 and, due to its lipophilic nature, effectively crosses mitochondrial membranes (10). Accordingly, elevating ABCB10 expression is sufficient to increase cytosolic and mitochondrial bilirubin content. Indeed, BLVRA can be associated with the cytosolic side of the ER (41, 42), an organelle with tight interactions with mitochondria in liver from insulin resistant mice (43). This tight interaction means that biliverdin exported by mitochondria can be readily transformed to bilirubin in ER-mitochondria contact areas, a microdomain that could facilitate a preferential trafficking of bilirubin to mitochondria.

Initially, we expected that hepatic ABCB10 deletion would exacerbate insulin resistance and steatosis in obese mice by increasing oxidative damage and disrupting insulin signaling (44, 45). However, we obtained the opposite results. Mitochondrial OXPHOS and insulin signaling were improved in hepatocytes from diet-induced obese ABCB10 LKO mice, concurrent with mild increases in mitochondrial and cytosolic H_2O_2 content. Our study is not the first example showing that a protein that hinders H_2O_2 actions in hepatocytes promotes insulin resistance and steatosis. Hepatocyte-specific deletion of glutathione peroxidase 1 (GPX1 LKO mice), a mitochondrial and cytosolic enzyme that removes H_2O_2, and hepatocyte-specific decreases in cytosolic biliverdin production achieved by deleting heme oxygenase 1 (HMOX1 LKO mice) induced the same benefits as ABCB10 deletion. In GPX1 LKO and HMOX1 LKO mice, an improvement in insulin sensitivity was explained by the post-translational oxidative inactivation of the phosphatase PTP1B (20, 36).

PTP1B is maladaptive in obesity, as it blocks insulin signaling transduction and promotes lipid synthesis in liver (37, 46). The increase in mitochondrial H_2O_2 release as a result of GPX1 and HMOX1 deletion leads to the oxidative inactivation of the catalytic cysteine in PTP1B. Hepatocyte-specific deletion or 50% downregulation of PTP1B activity is sufficient to protect mice from diet-induced obesity insulin resistance and steatosis (37, 46). Accordingly, we found that ABCB10 deletion decreased PTP1B phosphatase activity (30%) in hepatocytes from HFD fed mice, similarly to what was reported for GPX1 and HMOX1 deletion. However, the benefits induced by hepatic ABCB10 deletion on metabolic health are greater when compared to PTP1B deletion (37). These phenotypic differences support that ABCB10 deletion induces additional benefits beyond PTP1B inactivation. We propose that the increase in mitochondria function and energy expenditure observed in ABCB10

LKO mice are responsible for these additional benefits. In this regard, we demonstrated that decreased mitochondrial bilirubin content induced by ABCB10 deletion is responsible for improved mitochondrial function, a benefit that is not expected when PTP1B is deleted.

Other approaches inducing systemic increases in heme catabolism or in plasma bilirubin were shown to protect from metabolic dysfunction in obesity (47). However, mitochondrial bilirubin content was not measured in this study, meaning that it is possible that mitochondrial bilirubin was decreased by these other approaches. In this regard, bilirubin generated from mitochondrial biliverdin might preferentially act on different subcellular sites than imported bilirubin or bilirubin generated from cytosolic biliverdin. This preferential action could be achieved by confining bilirubin to a microdomain (ER-mitochondria contact areas) to restrict its action on specific targets. Thus, we propose that mechanisms controlling BLVRA trafficking to different cytosolic microdomains might be a major determinant of adapative and maladaptive bilirubin actions.

Controversy exists on whether bilirubin can be synthesized in the mitochondrial matrix, with one study detecting BLVRA in the inner mitochondrial membrane (48). This study did not determine whether the catalytic domain of BLVRA responsible for bilirubin synthesis was facing the matrix or the intermembrane space (IMS) (48). Indeed, the authors showed that isolated liver mitochondria can transform exogenous biliverdin to bilirubin. The transformation of exogenously added biliverdin supports that, if BLVRA was located in the inner membrane, the domain responsible for bilirubin synthesis could be facing the IMS to access exogenous biliverdin more easily. Moreover, it is unknown how BLVRA translocates from the cytosol to the inner membrane, as no mitochondrial targeting sequence is present in BLVRA. Last, other independent studies could not reproduce BLVRA detection in mitochondria, including MitoCarta (13, 14). Our data showing the existence of an active mitochondrial biliverdin export supports that bilirubin is not synthesized in the matrix. Lack of matrix bilirubin synthesis or in the inner membrane face of the IMS could be justified by the need to prevent bilirubin bursts damaging the mitochondrial inner membrane. Bilirubin is a lipophilic molecule that can strongly bind to membranes and fatty acid binding proteins. Indeed, bilirubin can make the membrane leaky to protons at low concentrations and completely block electron transfer at higher concentrations (12).

The maladaptive and non-essential role of hepatic ABCB10 function further supports that bilirubin is the major effector of ABCB10 actions. Bilirubin availability in hepatocytes *in vivo* cannot be severely impaired by eliminating ABCB10-mediated biliverdin export. ABCB10 KO hepatocytes can still synthesize bilirubin from biliverdin generated in the cytosol and import bilirubin from the blood (70% of bilirubin synthesis is extrahepatic) (9). Moreover, our data show that biliverdin accumulation in liver mitochondria induced by ABCB10 deletion is not toxic in mice. This conclusion can apply to erythroid cells as well, as the essential role of ABCB10 supporting heme synthesis in erythroid cells was rescued by antioxidant treatments (16). Consequently, heme biosynthesis and respiration occur in ABCB10 KO erythroid mitochondria accumulating biliverdin when oxidative damage is prevented. The role of bilirubin actions in erythroid cells remains largely uncharacterized, as the assumption is that heme molecules synthesized in erythroid mitochondria are all

exported to produce hemoglobin and none of them are degraded. Our study could potentially change our understanding of mitochondrial heme fate during erythroid differentiation.

As ABCB10 is dispensable for mouse liver function, is maladaptive in murine obesity, and its role exporting biliverdin and modulating insulin signaling is conserved in humans, we propose that hepatocyte-restricted targeting of ABCB10 holds promise as an approach to be tested to counteract hepatic insulin resistance and steatosis. The main limitation of our study is that the role of ABCB10 in mouse models of more severe forms of liver disease was not determined. Thus, it is a possibility that ABCB10 could be playing a protective role when liver damage is induced by something different than a high-fat diet model of obesity. In addition, the mechanism by which bilirubin slows down OXPHOS directly in mitochondria remains unidentified, but should involve saturable binding sites.

Materials and Methods

Study design.

The aim of this study was to examine the substrate transported by ABCB10, as well as the role of ABCB10 in the development of insulin resistance and steatosis. To this end, we used ABCB10 reconstituted into liposomes and nanodiscs, hepatocyte-specific ABCB10 KO mice, isolated mouse primary hepatocytes, human primary hepatocytes, and AML12 murine hepatocytes. We used fluorescent sensors to quantify bilirubin, H_2O_2, and GSSG/GSH in intact hepatocytes to determine the role of ABCB10 regulating the redox state and bilirubin compartmentalization in live cells. All experiments were approved by IACUC at Boston University and by ARC at UCLA. For mouse studies, a power analysis was used to calculate the sample sizes required. For *in vitro* studies, a minimum of three independent experiments were performed and the numbers of independent experiments (n) are presented in the figure legends.

Abcb10$^{Wt/flox}$ mice generation.

Targeted C57BL/6J ES cells with *Abcb10* containing loxP sites flanking exons 2–3 and a neomycin cassette flanked by Frt sites were generated by Genoway. Targeted ES cells were injected and implanted in C57BL/6J-Tyrc-2J/J (albino) females at the Boston University Mouse Transgenic Core, directed by Gregory L. Martin and Katya Ravid. Seven male chimeras containing floxed ABCB10 were identified by coat color and bred with C57BL/6J FLP recombinase females from Jackson (B6.Cg-Tg(ACTFLPe)9205Dym/J) to excise the neomycin cassette. The offspring were bred with wild type C57BL/6J, to obtain *Abcb10*$^{wt/flox}$ mice without FLP recombinase. *Abcb10*$^{wt/flox}$ mice were paired with B6.Cg-Tg(Alb-cre)21Mgn/J purchased from Jackson, to generate ABCB10 liver-specific KO mice. Groups analyzed were offspring littermates from breeding pairs between *Abcb10*$^{flox/flox}$; *Alb-Cre*$^{-/-}$ with *Abcb10*$^{wt/flox}$; *Alb-Cre*$^{+/-}$. Wild type mice (WT) are *Abcb10*$^{flox/flox}$ and *Abcb10*$^{wt/flox}$ mice (no Cre) and ABCB10-LKO are *Abcb10*$^{flox/flox}$; *Alb-Cre*$^{+/-}$.

Mice, diets, metabolic and body composition measurements

Mice were provided with water and food *ad libitum*, housed 2–5 mice per cage, 12h light:dark cycle and at a room temperature of 22–24ºC. Obesity and insulin resistance were

induced by high-fat diet feeding (D12451, Research Diets, 45 kcal % fat). Lean controls were mice fed a chow diet for the same period of time. Male mice were introduced to the diets after weaning (3–4 weeks of age). Body weight and food intake were monitored weekly. Glucose tolerance tests (GTT), Insulin tolerance tests (ITT) and metabolic cage measurements (CLAMS) were sequentially performed in the same cohorts of mice. Mice were left 2 weeks to recover between GTT and ITT measurements. ITTs were performed at 26 weeks and GTTs at 28 weeks of diet. At 30 weeks of diet, lean and fat mass were measured using Echo MRI, using a known mass of canola oil for calibration purposes, followed by 5 days of metabolic cage measurements. Additional cohorts of mice were used at 30 weeks to perform hyperinsulinemic-euglycemic clamps and isolate primary hepatocytes. Mice were left to recover from the metabolic cage analyses for 1 week and then euthanized, with plasma and tissues harvested for biochemical analyses. Body weight, GTT, ITT, and hyperinsulinemic clamps confirmed that protection from high-fat diet in LKO mice was preserved between 26–32 weeks of HFD feeding.

Statistical analyses

Data were tested for normality using Shapiro-Wilk. Excel, Graph Pad 8, and Sigma Plot 14.0 were used for statistical analyses, which included Student's t-tests or Mann-Whitney when comparing two groups, one-way ANOVA with Tukey or two-way ANOVA with Tukey or Holm-Sidak post hoc, when comparing multiple groups of samples. ANCOVA was performed with Sigma Plot 14, Systat Software Inc. using the MMPC website: https://www.mmpc.org/shared/regression.aspx. Chemical structures of bilirubin and biliverdin were taken from PubChem and drawn with ChemDoodle software.

Supplementary Material

Refer to Web version on PubMed Central for supplementary material.

ACKNOWLEDGEMENTS

We thank Daniel Braas and Thomas Graeber at the UCLA Metabolomics core for the LC/MS measurements of biliverdin. We thank Shinobu Matsuura, Gregory Martin, and Katya Ravid from the Transgenic Core at Boston University for the generation of ABCB10 floxed mice. We thank Tom Balon from Boston University for help with CLAMS. We thank Tobias Dick for the roGFP2 constructs, and thank Jong-Seok Park and Hyun-Woo Rhee for the UnaG construct. We thank Barbara E. Corkey, Marcus Fernandes de Oliveira, Susan K. Fried, and Orian S. Shirihai for input and discussions, and Sam B. Sereda, Eleni Ritou, and Nate Miller for technical assistance.

Funding:

M.L. is funded by the Department of Medicine at UCLA, pilot grants from P30 DK 41301 (UCLA:DDRC NIH), P50 AA011999 (USC-ALPD), UL1TR001881 (CTSI), P30 DK063491 (UCSD-UCLA DERC), P30 DK046200 (BNORC), and NIH-1R01AA026914-01A1. M.E.Z is funded by NIH-1R15GM131289-01. M.Sh. is funded by the Canadian Diabetes Association. C.A.S, R.A., M.R.Y, B.F. and E.P.C. were in the SGC, a registered charity funded by AbbVie, Bayer Pharma AG, Boehringer Ingelheim, Canada Foundation for Innovation, Genome Canada, Janssen, Merck KGaA, Merck & Co., Novartis, Ontario Ministry of Economic Development and Innovation, Pfizer, São Paulo Research Foundation-FAPESP, Takeda, Innovative Medicines Initiative Joint Undertaking ULTRA-DD grant 115766 and Wellcome Trust (106169/Z/14/Z). TA and JA were funded by by NIH 1R35GM135175-01, A.J.L by NIH-P01HL028481 and DK120342, and K.C.K by K99 DK120875 and AHA18POST33990256.

Data availability:

All data associated with this study are present in the paper or supplementary materials. The hybrid mouse diversity panel (HMDP) data is available at https://systems.genetics.ucla.edu. roGFP2 constructs were obtained under an MTA with Dr. Tobias Dick.

References and notes

1. Shadel GS, Horvath TL, Mitochondrial ROS signaling in organismal homeostasis. Cell 163, 560–569 (2015); published online EpubOct 22 (10.1016/j.cell.2015.10.001). [PubMed: 26496603]
2. Mironczuk-Chodakowska I, Witkowska AM, Zujko ME, Endogenous non-enzymatic antioxidants in the human body. Adv Med Sci 63, 68–78 (2018); published online EpubMar (10.1016/j.advms.2017.05.005). [PubMed: 28822266]
3. Sedlak TW, Saleh M, Higginson DS, Paul BD, Juluri KR, Snyder SH, Bilirubin and glutathione have complementary antioxidant and cytoprotective roles. Proc Natl Acad Sci U S A 106, 5171–5176 (2009); published online EpubMar 31 (10.1073/pnas.0813132106). [PubMed: 19286972]
4. Park JS, Nam E, Lee HK, Lim MH, Rhee HW, In Cellulo Mapping of Subcellular Localized Bilirubin. ACS Chem Biol 11, 2177–2185 (2016); published online EpubAug 19 (10.1021/acschembio.6b00017). [PubMed: 27232847]
5. Chiabrando D, Vinchi F, Fiorito V, Mercurio S, Tolosano E, Heme in pathophysiology: a matter of scavenging, metabolism and trafficking across cell membranes. Front Pharmacol 5, 61 (2014)10.3389/fphar.2014.00061).
6. Baranano DE, Rao M, Ferris CD, Snyder SH, Biliverdin reductase: a major physiologic cytoprotectant. Proc. Natl. Acad. Sci. U. S. A 99, 16093–16098 (2002); published online Epub12/10/2002 (10.1073/pnas.252626999 [doi];252626999 [pii]). [PubMed: 12456881]
7. Stocker R, Yamamoto Y, McDonagh AF, Glazer AN, Ames BN, Bilirubin is an antioxidant of possible physiological importance. Science 235, 1043–1046 (1987); published online Epub2/27/1987 ([PubMed: 3029864]
8. Nytofte NS, Serrano MA, Monte MJ, Gonzalez-Sanchez E, Tumer Z, Ladefoged K, Briz O, Marin JJ, A homozygous nonsense mutation (c.214C->A) in the biliverdin reductase alpha gene (BLVRA) results in accumulation of biliverdin during episodes of cholestasis. J Med Genet 48, 219–225 (2011); published online EpubApr (10.1136/jmg.2009.074567). [PubMed: 21278388]
9. Erlinger S, Arias IM, Dhumeaux D, Inherited disorders of bilirubin transport and conjugation: new insights into molecular mechanisms and consequences. Gastroenterology 146, 1625–1638 (2014); published online Epub6/2014 (S0016–5085(14)00444–2 [pii];10.1053/j.gastro.2014.03.047 [doi]). [PubMed: 24704527]
10. Zucker SD, Goessling W, Hoppin AG, Unconjugated bilirubin exhibits spontaneous diffusion through model lipid bilayers and native hepatocyte membranes. J Biol Chem 274, 10852–10862 (1999); published online EpubApr 16 (10.1074/jbc.274.16.10852). [PubMed: 10196162]
11. Schutta HS, Johnson L, Neville HE, Mitochondrial abnormalities in bilirubin encephalopathy. J Neuropathol Exp Neurol 29, 296–305 (1970); published online EpubApr (10.1097/00005072-197004000-00010). [PubMed: 5435823]
12. Mustafa MG, Cowger ML, King TE, Effects of bilirubin on mitochondrial reactions. J. Biol. Chem 244, 6403–6414 (1969); published online Epub12/10/1969 ([PubMed: 4982202]
13. Slebos DJ, Ryter SW, van der Toorn M, Liu F, Guo F, Baty CJ, Karlsson JM, Watkins SC, Kim HP, Wang X, Lee JS, Postma DS, Kauffman HF, Choi AM, Mitochondrial localization and function of heme oxygenase-1 in cigarette smoke-induced cell death. Am J Respir Cell Mol Biol 36, 409–417 (2007); published online EpubApr (10.1165/rcmb.2006-0214OC). [PubMed: 17079780]
14. Calvo SE, Clauser KR, Mootha VK, MitoCarta2.0: an updated inventory of mammalian mitochondrial proteins. Nucleic Acids Res 44, D1251–1257 (2016); published online EpubJan 4 (10.1093/nar/gkv1003). [PubMed: 26450961]
15. Chen W, Paradkar PN, Li L, Pierce EL, Langer NB, Takahashi-Makise N, Hyde BB, Shirihai OS, Ward DM, Kaplan J, Paw BH, Abcb10 physically interacts with mitoferrin-1 (Slc25a37) to

enhance its stability and function in the erythroid mitochondria. Proc. Natl. Acad. Sci. U. S. A 106, 16263–16268 (2009); published online Epub9/22/2009 (0904519106 [pii];10.1073/pnas.0904519106 [doi]). [PubMed: 19805291]

16. Hyde BB, Liesa M, Elorza AA, Qiu W, Haigh SE, Richey L, Mikkola HK, Schlaeger TM, Shirihai OS, The mitochondrial transporter ABC-me (ABCB10), a downstream target of GATA-1, is essential for erythropoiesis in vivo. Cell Death. Differ 19, 1117–1126 (2012); published online Epub7/2012 (cdd2011195 [pii];10.1038/cdd.2011.195 [doi]). [PubMed: 22240895]
17. Yamamoto M, Arimura H, Fukushige T, Minami K, Nishizawa Y, Tanimoto A, Kanekura T, Nakagawa M, Akiyama S, Furukawa T, Abcb10 role in heme biosynthesis in vivo: Abcb10 knockout in mice causes anemia with protoporphyrin IX and iron accumulation. Mol. Cell Biol 34, 1077–1084 (2014); published online Epub3/2014 (MCB.00865–13 [pii];10.1128/MCB.00865-13 [doi]). [PubMed: 24421385]
18. Tang L, Bergevoet SM, Bakker-Verweij G, Harteveld CL, Giordano PC, Nijtmans L, de Witte T, Jansen JH, Raymakers RA, van der Reijden BA, Human mitochondrial ATP-binding cassette transporter ABCB10 is required for efficient red blood cell development. Br J Haematol 157, 151–154 (2012); published online EpubApr (10.1111/j.1365-2141.2011.08936.x). [PubMed: 22085049]
19. Bonkowsky HL, Sinclair PR, Sinclair JF, Hepatic heme metabolism and its control. Yale J Biol Med 52, 13–37 (1979); published online EpubJan-Feb ([PubMed: 222077]
20. Jais A, Einwallner E, Sharif O, Gossens K, Lu TT, Soyal SM, Medgyesi D, Neureiter D, Paier-Pourani J, Dalgaard K, Duvigneau JC, Lindroos-Christensen J, Zapf TC, Amann S, Saluzzo S, Jantscher F, Stiedl P, Todoric J, Martins R, Oberkofler H, Muller S, Hauser-Kronberger C, Kenner L, Casanova E, Sutterluty-Fall H, Bilban M, Miller K, Kozlov AV, Krempler F, Knapp S, Lumeng CN, Patsch W, Wagner O, Pospisilik JA, Esterbauer H, Heme oxygenase-1 drives metaflammation and insulin resistance in mouse and man. Cell 158, 25–40 (2014); published online EpubJul 3 (10.1016/j.cell.2014.04.043). [PubMed: 24995976]
21. Mahajan A, Taliun D, Thurner M, Robertson NR, Torres JM, Rayner NW, Payne AJ, Steinthorsdottir V, Scott RA, Grarup N, Cook JP, Schmidt EM, Wuttke M, Sarnowski C, Magi R, Nano J, Gieger C, Trompet S, Lecoeur C, Preuss MH, Prins BP, Guo X, Bielak LF, Below JE, Bowden DW, Chambers JC, Kim YJ, Ng MCY, Petty LE, Sim X, Zhang W, Bennett AJ, Bork-Jensen J, Brummett CM, Canouil M, Ec Kardt KU, Fischer K, Kardia SLR, Kronenberg F, Lall K, Liu CT, Locke AE, Luan J, Ntalla I, Nylander V, Schonherr S, Schurmann C, Yengo L, Bottinger EP, Brandslund I, Christensen C, Dedoussis G, Florez JC, Ford I, Franco OH, Frayling TM, Giedraitis V, Hackinger S, Hattersley AT, Herder C, Ikram MA, Ingelsson M, Jorgensen ME, Jorgensen T, Kriebel J, Kuusisto J, Ligthart S, Lindgren CM, Linneberg A, Lyssenko V, Mamakou V, Meitinger T, Mohlke KL, Morris AD, Nadkarni G, Pankow JS, Peters A, Sattar N, Stancakova A, Strauch K, Taylor KD, Thorand B, Thorleifsson G, Thorsteinsdottir U, Tuomilehto J, Witte DR, Dupuis J, Peyser PA, Zeggini E, Loos RJF, Froguel P, Ingelsson E, Lind L, Groop L, Laakso M, Collins FS, Jukema JW, Palmer CNA, Grallert H, Metspalu A, Dehghan A, Kottgen A, Abecasis GR, Meigs JB, Rotter JI, Marchini J, Pedersen O, Hansen T, Langenberg C, Wareham NJ, Stefansson K, Gloyn AL, Morris AP, Boehnke M, McCarthy MI, Fine-mapping type 2 diabetes loci to single-variant resolution using high-density imputation and islet-specific epigenome maps. Nat Genet 50, 1505–1513 (2018); published online EpubNov (10.1038/s41588-018-0241-6). [PubMed: 30297969]
22. Morris AP, Voight BF, Teslovich TM, Ferreira T, Segre AV, Steinthorsdottir V, Strawbridge RJ, Khan H, Grallert H, Mahajan A, Prokopenko I, Kang HM, Dina C, Esko T, Fraser RM, Kanoni S, Kumar A, Lagou V, Langenberg C, Luan J, Lindgren CM, Muller-Nurasyid M, Pechlivanis S, Rayner NW, Scott LJ, Wiltshire S, Yengo L, Kinnunen L, Rossin EJ, Raychaudhuri S, Johnson AD, Dimas AS, Loos RJ, Vedantam S, Chen H, Florez JC, Fox C, Liu CT, Rybin D, Couper DJ, Kao WH, Li M, Cornelis MC, Kraft P, Sun Q, van Dam RM, Stringham HM, Chines PS, Fischer K, Fontanillas P, Holmen OL, Hunt SE, Jackson AU, Kong A, Lawrence R, Meyer J, Perry JR, Platou CG, Potter S, Rehnberg E, Robertson N, Sivapalaratnam S, Stancakova A, Stirrups K, Thorleifsson G, Tikkanen E, Wood AR, Almgren P, Atalay M, Benediktsson R, Bonnycastle LL, Burtt N, Carey J, Charpentier G, Crenshaw AT, Doney AS, Dorkhan M, Edkins S, Emilsson V, Eury E, Forsen T, Gertow K, Gigante B, Grant GB, Groves CJ, Guiducci C, Herder C, Hreidarsson AB, Hui J, James A, Jonsson A, Rathmann W, Klopp N, Kravic J, Krjutskov K, Langford C, Leander K, Lindholm E, Lobbens S, Mannisto S, Mirza G, Muhleisen TW, Musk B, Parkin M,

Rallidis L, Saramies J, Sennblad B, Shah S, Sigurethsson G, Silveira A, Steinbach G, Thorand B, Trakalo J, Veglia F, Wennauer R, Winckler W, Zabaneh D, Campbell H, van Duijn C, Uitterlinden AG, Hofman A, Sijbrands E, Abecasis GR, Owen KR, Zeggini E, Trip MD, Forouhi NG, Syvanen AC, Eriksson JG, Peltonen L, Nothen MM, Balkau B, Palmer CN, Lyssenko V, Tuomi T, Isomaa B, Hunter DJ, Qi L, Wellcome C Trust Case Control, G. Meta-Analyses of, I. Insulin-related traits Consortium, A. T. C. Genetic Investigation of, C. Asian Genetic Epidemiology Network-Type 2 Diabetes, C. South Asian Type 2 Diabetes, Shuldiner AR, Roden M, Barroso I, Wilsgaard T, Beilby J, Hovingh K, Price JF, Wilson JF, Rauramaa R, Lakka TA, Lind L, Dedoussis G, Njolstad I, Pedersen NL, Khaw KT, Wareham NJ, Keinanen-Kiukaanniemi SM, Saaristo TE, Korpi-Hyovalti E, Saltevo J, Laakso M, Kuusisto J, Metspalu A, Collins FS, Mohlke KL, Bergman RN, Tuomilehto J, Boehm BO, Gieger C, Hveem K, Cauchi S, Froguel P, Baldassarre D, Tremoli E, Humphries SE, Saleheen D, Danesh J, Ingelsson E, Ripatti S, Salomaa V, Erbel R, Jockel KH, Moebus S, Peters A, Illig T, de Faire U, Hamsten A, Morris AD, Donnelly PJ, Frayling TM, Hattersley AT, Boerwinkle E, Melander O, Kathiresan S, Nilsson PM, Deloukas P, Thorsteinsdottir U, Groop LC, Stefansson K, Hu F, Pankow JS, Dupuis J, Meigs JB, Altshuler D, Boehnke M, McCarthy MI, Replication DIG, Meta-analysis C, Large-scale association analysis provides insights into the genetic architecture and pathophysiology of type 2 diabetes. Nat Genet 44, 981–990 (2012); published online EpubSep (10.1038/ng.2383). [PubMed: 22885922]

23. Seguin A, Takahashi-Makise N, Yien YY, Huston NC, Whitman JC, Musso G, Wallace JA, Bradley T, Bergonia HA, Kafina MD, Matsumoto M, Igarashi K, Phillips JD, Paw BH, Kaplan J, Ward DM, Reductions in the mitochondrial ABC transporter Abcb10 affect the transcriptional profile of heme biosynthesis genes. J Biol Chem 292, 16284–16299 (2017); published online EpubSep 29 (10.1074/jbc.M117.797415). [PubMed: 28808058]
24. Qiu W, Liesa M, Carpenter EP, Shirihai OS, ATP Binding and Hydrolysis Properties of ABCB10 and Their Regulation by Glutathione. PLoS One 10, e0129772 (2015)10.1371/journal.pone.0129772). [PubMed: 26053025]
25. Shintre CA, Pike AC, Li Q, Kim JI, Barr AJ, Goubin S, Shrestha L, Yang J, Berridge G, Ross J, Stansfeld PJ, Sansom MS, Edwards AM, Bountra C, Marsden BD, von Delft F, Bullock AN, Gileadi O, Burgess-Brown NA, Carpenter EP, Structures of ABCB10, a human ATP-binding cassette transporter in apo- and nucleotide-bound states. Proc Natl Acad Sci U S A 110, 9710–9715 (2013); published online EpubJun 11 (10.1073/pnas.1217042110). [PubMed: 23716676]
26. Martinez M, Fendley GA, Saxberg AD, Zoghbi ME, Stimulation of the human mitochondrial transporter ABCB10 by zinc-mesoporphrin. PLoS One 15, e0238754 (2020)10.1371/journal.pone.0238754). [PubMed: 33253225]
27. Saxberg AD, Martinez M, Fendley GA, Zoghbi ME, Production of a human mitochondrial ABC transporter in E. coli. Protein Expr Purif 178, 105778 (2021); published online EpubFeb (10.1016/j.pep.2020.105778). [PubMed: 33069825]
28. Kumagai A, Ando R, Miyatake H, Greimel P, Kobayashi T, Hirabayashi Y, Shimogori T, Miyawaki A, A bilirubin-inducible fluorescent protein from eel muscle. Cell 153, 1602–1611 (2013); published online EpubJun 20 (10.1016/j.cell.2013.05.038). [PubMed: 23768684]
29. Bennett BJ, Davis RC, Civelek M, Orozco L, Wu J, Qi H, Pan C, Packard RR, Eskin E, Yan M, Kirchgessner T, Wang Z, Li X, Gregory JC, Hazen SL, Gargalovic PS, Lusis AJ, Genetic Architecture of Atherosclerosis in Mice: A Systems Genetics Analysis of Common Inbred Strains. PLoS Genet 11, e1005711 (2015); published online EpubDec (10.1371/journal.pgen.1005711). [PubMed: 26694027]
30. Shirihai OS, Gregory T, Yu C, Orkin SH, Weiss MJ, ABC-me: a novel mitochondrial transporter induced by GATA-1 during erythroid differentiation. EMBO J 19, 2492–2502 (2000); published online Epub6/1/2000 (10.1093/emboj/19.11.2492 [doi]). [PubMed: 10835348]
31. Perry RJ, Samuel VT, Petersen KF, Shulman GI, The role of hepatic lipids in hepatic insulin resistance and type 2 diabetes. Nature 510, 84–91 (2014); published online EpubJun 5 (10.1038/nature13478). [PubMed: 24899308]
32. Michael MD, Kulkarni RN, Postic C, Previs SF, Shulman GI, Magnuson MA, Kahn CR, Loss of insulin signaling in hepatocytes leads to severe insulin resistance and progressive hepatic dysfunction. Mol. Cell 6, 87–97 (2000); published online Epub7/2000 (S1097–2765(05)00015–8 [pii]). [PubMed: 10949030]

33. Perry RJ, Camporez JG, Kursawe R, Titchenell PM, Zhang D, Perry CJ, Jurczak MJ, Abudukadier A, Han MS, Zhang XM, Ruan HB, Yang X, Caprio S, Kaech SM, Sul HS, Birnbaum MJ, Davis RJ, Cline GW, Petersen KF, Shulman GI, Hepatic acetyl CoA links adipose tissue inflammation to hepatic insulin resistance and type 2 diabetes. Cell 160, 745–758 (2015); published online EpubFeb 12 (10.1016/j.cell.2015.01.012). [PubMed: 25662011]
34. Vernia S, Cavanagh-Kyros J, Garcia-Haro L, Sabio G, Barrett T, Jung DY, Kim JK, Xu J, Shulha HP, Garber M, Gao G, Davis RJ, The PPARalpha-FGF21 hormone axis contributes to metabolic regulation by the hepatic JNK signaling pathway. Cell Metab 20, 512–525 (2014); published online EpubSep 2 (10.1016/j.cmet.2014.06.010). [PubMed: 25043817]
35. Perry RJ, Kim T, Zhang XM, Lee HY, Pesta D, Popov VB, Zhang D, Rahimi Y, Jurczak MJ, Cline GW, Spiegel DA, Shulman GI, Reversal of hypertriglyceridemia, fatty liver disease, and insulin resistance by a liver-targeted mitochondrial uncoupler. Cell Metab 18, 740–748 (2013); published online EpubNov 5 (10.1016/j.cmet.2013.10.004). [PubMed: 24206666]
36. Merry TL, Tran M, Dodd GT, Mangiafico SP, Wiede F, Kaur S, McLean CL, Andrikopoulos S, Tiganis T, Hepatocyte glutathione peroxidase-1 deficiency improves hepatic glucose metabolism and decreases steatohepatitis in mice. Diabetologia 59, 2632–2644 (2016); published online EpubDec (10.1007/s00125-016-4084-3). [PubMed: 27628106]
37. Delibegovic M, Zimmer D, Kauffman C, Rak K, Hong EG, Cho YR, Kim JK, Kahn BB, Neel BG, Bence KK, Liver-specific deletion of protein-tyrosine phosphatase 1B (PTP1B) improves metabolic syndrome and attenuates diet-induced endoplasmic reticulum stress. Diabetes 58, 590–599 (2009); published online EpubMar (10.2337/db08-0913). [PubMed: 19074988]
38. Krishnan N, Bonham CA, Rus IA, Shrestha OK, Gauss CM, Haque A, Tocilj A, Joshua-Tor L, Tonks NK, Harnessing insulin- and leptin-induced oxidation of PTP1B for therapeutic development. Nat Commun 9, 283 (2018); published online EpubJan 18 (10.1038/s41467-017-02252-2). [PubMed: 29348454]
39. Shimizu S, Ugi S, Maegawa H, Egawa K, Nishio Y, Yoshizaki T, Shi K, Nagai Y, Morino K, Nemoto K, Nakamura T, Bryer-Ash M, Kashiwagi A, Protein-tyrosine phosphatase 1B as new activator for hepatic lipogenesis via sterol regulatory element-binding protein-1 gene expression. J Biol Chem 278, 43095–43101 (2003); published online EpubOct 31 (10.1074/jbc.M306880200). [PubMed: 12941932]
40. Mahadev K, Zilbering A, Zhu L, Goldstein BJ, Insulin-stimulated hydrogen peroxide reversibly inhibits protein-tyrosine phosphatase 1b in vivo and enhances the early insulin action cascade. J Biol Chem 276, 21938–21942 (2001); published online EpubJun 15 (10.1074/jbc.C100109200). [PubMed: 11297536]
41. Kutty RK, Maines MD, Purification and characterization of biliverdin reductase from rat liver. J. Biol. Chem 256, 3956–3962 (1981); published online Epub4/25/1981 ([PubMed: 7217067]
42. Yoshinaga T, Sassa S, Kappas A, The occurrence of molecular interactions among NADPH-cytochrome c reductase, heme oxygenase, and biliverdin reductase in heme degradation. J Biol Chem 257, 7786–7793 (1982); published online EpubJul 10 ([PubMed: 6806283]
43. Arruda AP, Pers BM, Parlakgul G, Guney E, Inouye K, Hotamisligil GS, Chronic enrichment of hepatic endoplasmic reticulum-mitochondria contact leads to mitochondrial dysfunction in obesity. Nat Med 20, 1427–1435 (2014); published online EpubDec (10.1038/nm.3735). [PubMed: 25419710]
44. Koliaki C, Szendroedi J, Kaul K, Jelenik T, Nowotny P, Jankowiak F, Herder C, Carstensen M, Krausch M, Knoefel WT, Schlensak M, Roden M, Adaptation of hepatic mitochondrial function in humans with non-alcoholic fatty liver is lost in steatohepatitis. Cell Metab 21, 739–746 (2015); published online EpubMay 5 (10.1016/j.cmet.2015.04.004). [PubMed: 25955209]
45. Sunny NE, Parks EJ, Browning JD, Burgess SC, Excessive hepatic mitochondrial TCA cycle and gluconeogenesis in humans with nonalcoholic fatty liver disease. Cell Metab 14, 804–810 (2011); published online EpubDec 7 (10.1016/j.cmet.2011.11.004). [PubMed: 22152305]
46. Agouni A, Mody N, Owen C, Czopek A, Zimmer D, Bentires-Alj M, Bence KK, Delibegovic M, Liver-specific deletion of protein tyrosine phosphatase (PTP) 1B improves obesity- and pharmacologically induced endoplasmic reticulum stress. Biochem. J 438, 369–378 (2011); published online Epub9/1/2011 (BJ20110373 [pii];10.1042/BJ20110373 [doi]). [PubMed: 21605081]

47. Liu J, Dong H, Zhang Y, Cao M, Song L, Pan Q, Bulmer A, Adams DB, Dong X, Wang H, Bilirubin Increases Insulin Sensitivity by Regulating Cholesterol Metabolism, Adipokines and PPARgamma Levels. Sci. Rep 5, 9886 (2015); published online Epub5/28/2015 (srep09886 [pii];10.1038/srep09886 [doi]). [PubMed: 26017184]

48. Converso DP, Taille C, Carreras MC, Jaitovich A, Poderoso JJ, Boczkowski J, HO-1 is located in liver mitochondria and modulates mitochondrial heme content and metabolism. FASEB J 20, 1236–1238 (2006); published online EpubJun (10.1096/fj.05-4204fje). [PubMed: 16672635]

49. Folch J, Lees M, Sloane Stanley GH, A simple method for the isolation and purification of total lipides from animal tissues. J Biol Chem 226, 497–509 (1957). [PubMed: 13428781]

50. Ribas V, Drew BG, Zhou Z, Phun J, Kalajian NY, Soleymani T, Daraei P, Widjaja K, Wanagat J, de Aguiar Vallim TQ, Fluitt AH, Bensinger S, Le T, Radu C, Whitelegge JP, Beaven SW, Tontonoz P, Lusis AJ, Parks BW, Vergnes L, Reue K, Singh H, Bopassa JC, Toro L, Stefani E, Watt MJ, Schenk S, Akerstrom T, Kelly M, Pedersen BK, Hewitt SC, Korach KS, Hevener AL, Skeletal muscle action of estrogen receptor alpha is critical for the maintenance of mitochondrial function and metabolic homeostasis in females. Science translational medicine 8, 334ra354 (2016).

51. Steele R, Influences of glucose loading and of injected insulin on hepatic glucose output. Annals of the New York Academy of Sciences 82, 420–430 (1959). [PubMed: 13833973]

52. Nocito L, Kleckner AS, Yoo EJ, Jones IV AR, Liesa M, Corkey BE, The extracellular redox state modulates mitochondrial function, gluconeogenesis, and glycogen synthesis in murine hepatocytes. PLoS. One 10, e0122818 (2015). [PubMed: 25816337]

53. Shum M, Bellmann K, St-Pierre P, Marette A, Pharmacological inhibition of S6K1 increases glucose metabolism and Akt signalling in vitro and in diet-induced obese mice. Diabetologia 59, 592–603 (2016). [PubMed: 26733005]

54. Meyer AJ, Dick TP, Fluorescent protein-based redox probes. Antioxid Redox Signal 13, 621–650 (2010). [PubMed: 20088706]

55. Mahdaviani K, Benador IY, Shu S, Gharakhanian RA, Stiles L, Trudeau KM, Cardamone M, Enríquez-Zarralanga V, Ritou E, Aprahamian T, Oliveira MF, Corkey BE, Liesa M, Shirihai OS, Mfn2 deletion in brown adipose tissue protects from insulin resistance and impairs thermogenesis. EMBO Rep 18, 1123–1138 (2017). [PubMed: 28539390]

56. Zoghbi ME, Cooper RS, Altenberg GA, The Lipid Bilayer Modulates the Structure and Function of an ATP-binding Cassette Exporter. J Biol Chem 291, 4453–4461 (2016). [PubMed: 26725230]

57. Geertsma ER, Nik Mahmood NA, Schuurman-Wolters GK, Poolman B, Membrane reconstitution of ABC transporters and assays of translocator function. Nat Protoc 3, 256–266 (2008). [PubMed: 18274528]

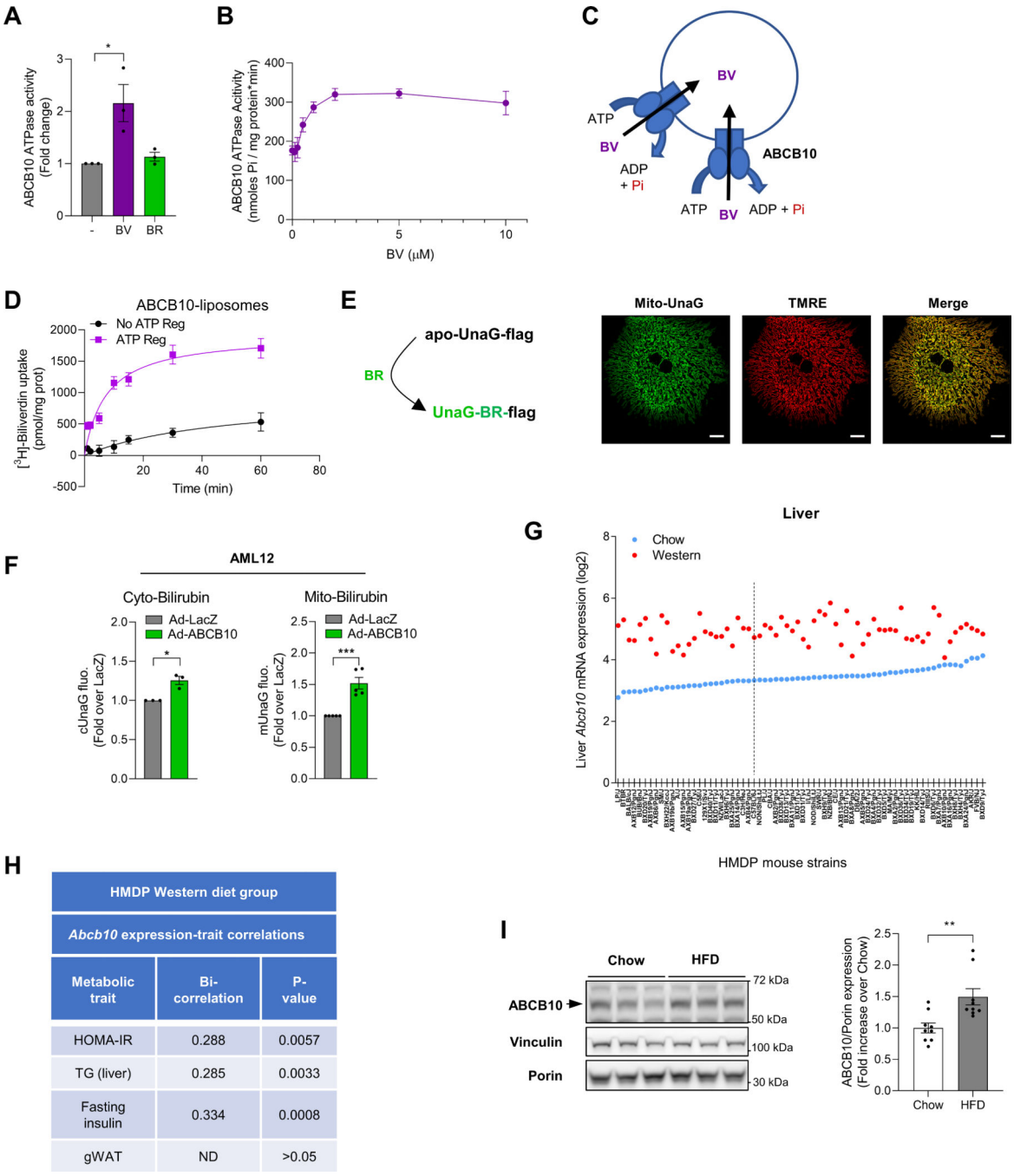

HMDP Western diet group		
Abcb10 expression-trait correlations		
Metabolic trait	Bi-correlation	P-value
HOMA-IR	0.288	0.0057
TG (liver)	0.285	0.0033
Fasting insulin	0.334	0.0008
gWAT	ND	>0.05

Fig. 1. ABCB10 exports mitochondrial biliverdin to increase bilirubin synthesis and is positively associated with insulin resistance and steatosis.

(**A**) ATPase activity of ABCB10 reconstituted into nanodiscs in the presence of biliverdin (BV, 5 μM) or bilirubin (BR, 5 μM). n=3 independent experiments. (**B**) Michaelis-Menten plot of ABCB10 ATPase activity with increasing biliverdin concentrations. N=7 independent experiments. (**C**) Scheme of ABCB10 orientation in sealed liposomes. (**D**) ^{3}[H]-biliverdin accumulation into sealed ABCB10-liposomes determined with or without ATP for the indicated times. Graph plotted using one-phase association equation, mean of n=5

independent transport experiments ± SEM, from two independent protein and liposome preparations. (**E**) UnaG-Flag protein fluorescence upon reversible binding to bilirubin, with high-resolution confocal images of primary mouse hepatocytes expressing the bilirubin sensor in mitochondria (Mito-UnaG or mUnaG) showing co-localization with the mitochondrial dye TMRE. Scale bar, 20 μm. (**F**) AML12 mouse hepatocytes co-transduced with adenovirus encoding LacZ or ABCB10 with cytosolic UnaG (cUnaG) or mUnaG to measure bilirubin, n=3–5 independent experiments. **(G)** Hepatic *Abcb10* mRNA content measured in 68 strains (x axis) of the Hybrid Mouse Diversity Panel (HMDP) fed chow (blue) or Western diet (red), including C57BL/6J (dashed line). (**H**) Biweight midcorrelation values between hepatic ABCB10 transcript content with the metabolic trait measured in the Western diet-fed HMDP mice, with nominal p values shown (n=102 strains). (**I**) ABCB10 expression in liver lysates from WT mice fed a HFD (45% Kcal as fat). n=9 mice per group; Mann-Whitney U test; *p<0.05; **p<0.01; ***p<0.001.

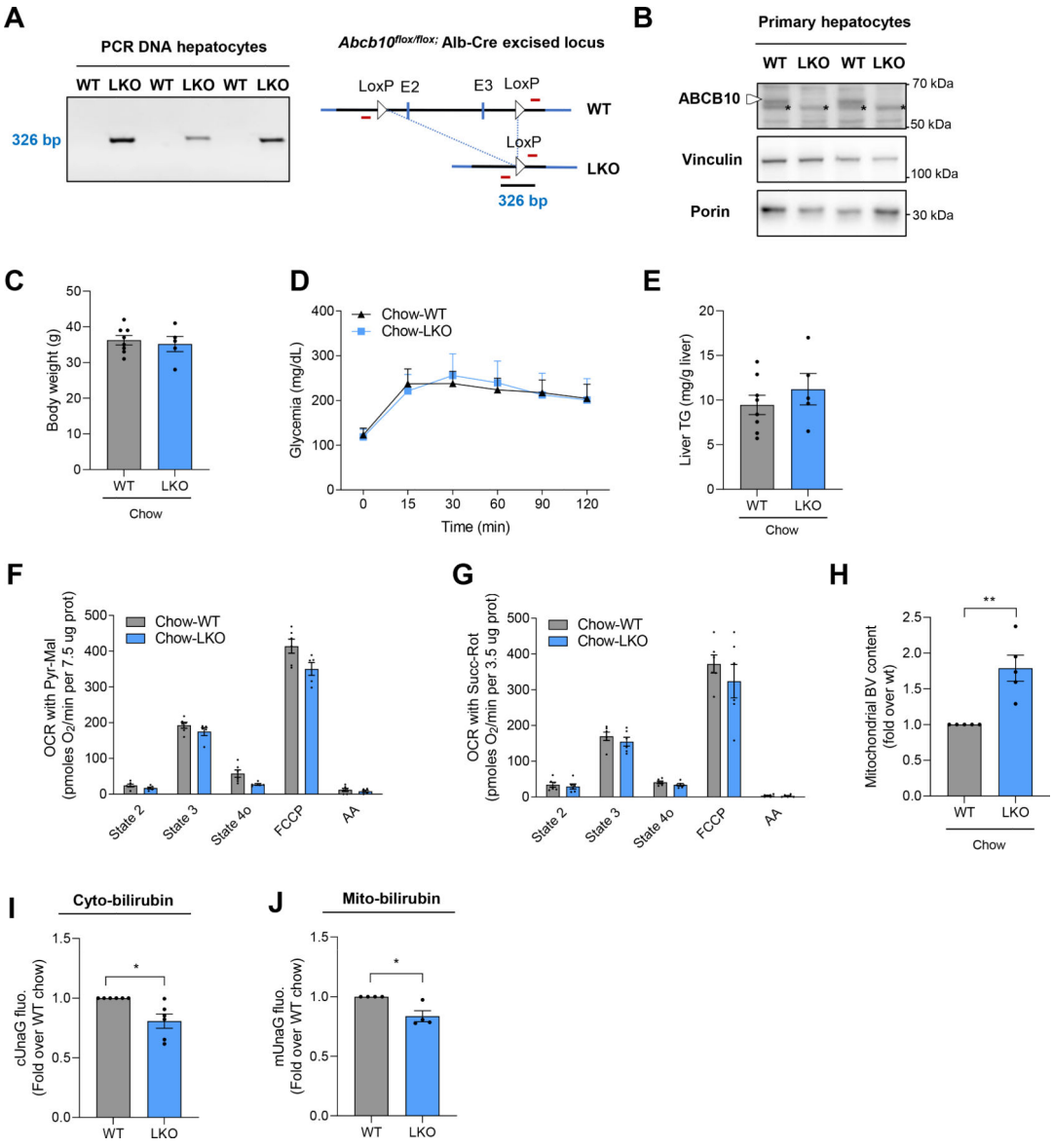

Fig. 2. ABCB10-mediated bilirubin synthesis is dispensable for normal hepatocyte function in control mice.

(**A**) PCR product of the genomic fragment resulting from Cre-mediated excision of *Abcb10*$^{flox/flox}$, determined in extracts of hepatocytes isolated from ABCB10-LKO mice; one mouse per lane. (**B**) ABCB10 protein measured in lysates from isolated primary hepatocytes, with an unspecific band close to ABCB10 marked with an asterisk*, one mouse per lane. Measurements in WT and ABCB10-LKO mice after 28 weeks of chow diet of (**C**) body weight and (**D**) blood glucose content during an i.p. glucose tolerance test (GTT) after 16h fast. n=5–8 male mice. (**E**) Liver triglyceride (TG) content in total liver lipid extracts. (**F-G**) Oxygen consumption rates (OCR) of isolated liver mitochondria from WT and ABCB10 LKO littermates under state 2 (leak), state 3 (maximal ATP synthesis), state 4o (leak after oligomycin injection), maximal respiratory capacity (FCCP), and non-respiration OCR (antimycin A, AA), fueled by pyruvate + malate (**F**) or by succinate + rotenone **(G)**.

n=5–6 mice/group. **(H)** Mitochondrial biliverdin content measured by LC/MS in liver mitochondria isolated from WT and ABCB10 LKO. n=5 mice/group. Student's t-test **p<0.01 (**I**) Primary hepatocytes from lean (chow diet) WT or ABCB10-LKO mice transduced with adenovirus encoding cytosolic UnaG (cUnaG), to measure cytosolic bilirubin content (Student's t-test; *p<0.05) or (**J**) with adenovirus encoding mitochondrial matrix-targeted UnaG (mUnaG). Mann-Whitney U test; *p<0.05. n=4–6 mice. Results are presented as mean ± SEM.

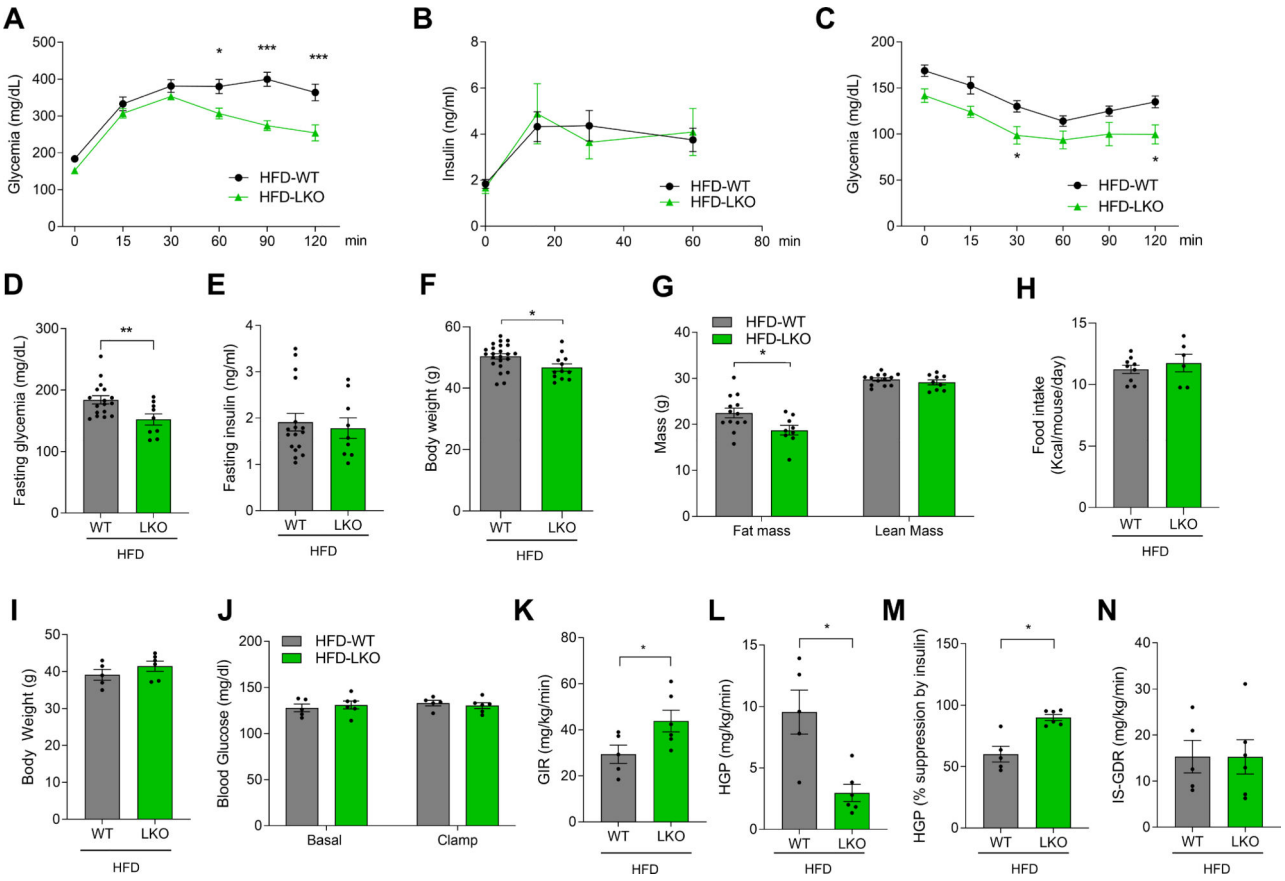

Fig. 3. Hepatic ABCB10 deletion protects from HFD-induced insulin resistance and increases insulin-mediated suppression of hepatic glucose production.

(A-N) WT and ABCB10 LKO male mice were fed a HFD and (**A**) blood glucose and (**B**) plasma insulin were measured after 16h fasting during GTT at 28 weeks of diet; Two-way ANOVA; *p<0.05, ***p<0.001, n=9–17 mice per group. (**C**) Insulin tolerance test (ITT) performed after a 6h fast at 26 weeks of HFD. Two-way ANOVA; *p<0.05, n=11–19 mice per group. (**D**) Fasting glycemia and (**E**), fasting insulinemia values from panels A and B. (**F**) Body weight of WT and LKO mice after 30 weeks of HFD. N=9–23 mice per group; Student's t-test, *p < 0.05 **p<0.01. (**G**) Lean and fat mass of HFD-fed WT and LKO mice determined by Echo-MRI at 30 weeks of diet. N=9–13 mice/group Student's t-test, *p < 0.05. (**H**) Daily food intake in WT or ABCB10 LKO mice. (**I-N**), Hyperinsulinemic-euglycemic clamps in weight-matched HFD-fed WT and ABCB10-LKO mice at 30 weeks of diet, n=5–6 mice/group. (**I**) Body weight of clamped mice with (**J**) blood glucose concentration at basal state and during the clamps. (**K**) Glucose infusion rates (GIR), Student's t-test, *p<0.05. (**L**) Hepatic glucose production (HGP), Student's t-test, *p<0.05. (**M**) Insulin suppression of HGP, Student's t-test, *p<0.05. (**N**), Insulin-stimulated glucose disappearance rate (IS-GDR). Results are presented as mean ± SEM.

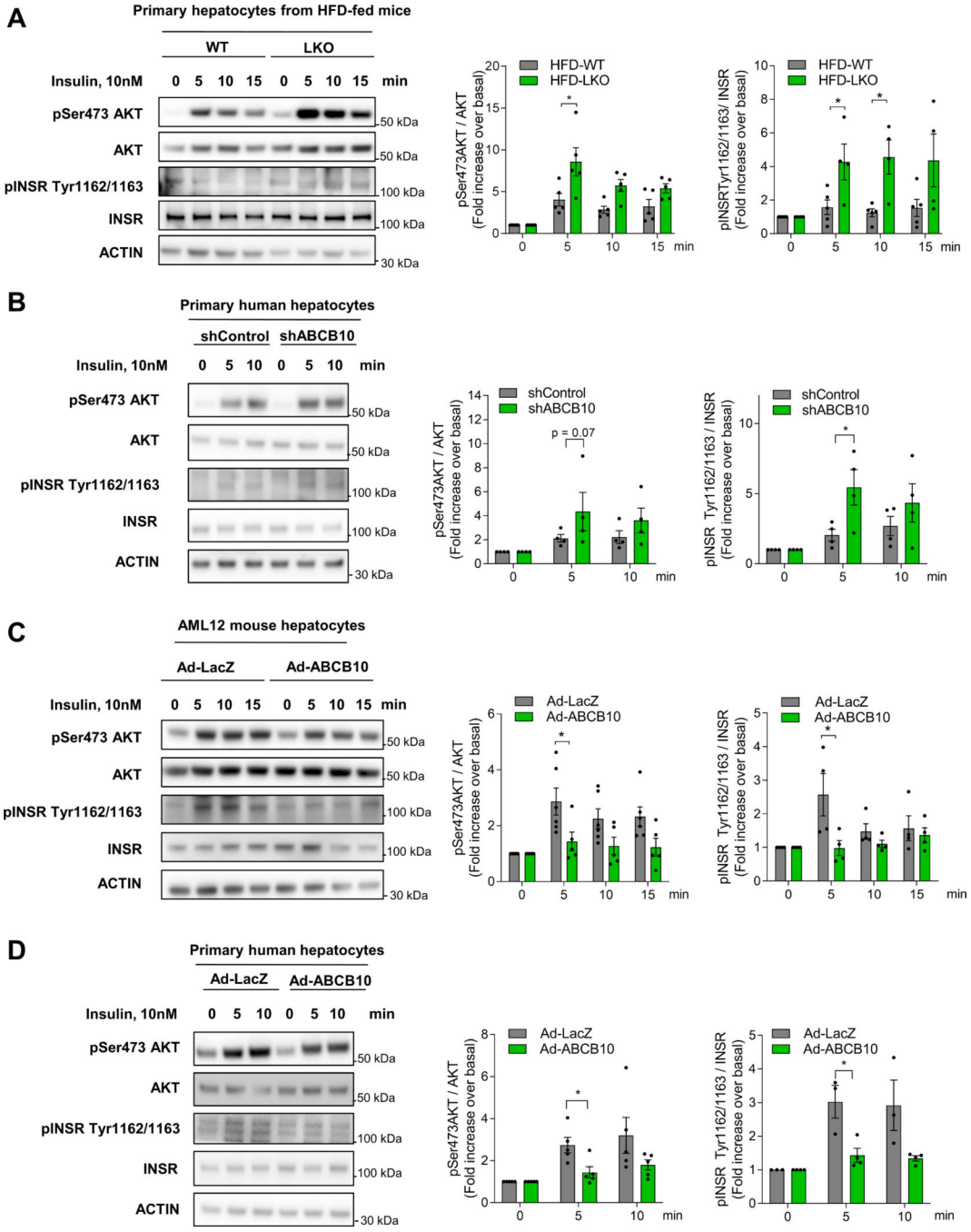

Fig. 4. ABCB10 is sufficient to impair insulin signaling in mouse and human primary hepatocytes.

(**A**) Western blots detecting pSer473 AKT and pTyr1162/1163 INSR in total lysates of primary hepatocytes isolated from HFD-fed WT and LKO mice. Hepatocytes were serum-starved (o/n) and treated with 10 nM insulin for the indicated times. n=4–5 independent experiments. (**B**) Human hepatocytes were transduced with lentivirus encoding shControl (sh001) or shABCB10. Two days after transduction, hepatocytes were serum-starved (6h) and treated with 10 nM insulin for the indicated times. Western blots of pSer473 AKT and

pIR Tyr1162/1163 in total lysates. n=4 independent experiments. (**C**) Mouse AML12 hepatocytes were transduced with Adenovirus (Ad) encoding LacZ or ABCB10. Two days after transduction, hepatocytes were serum-starved (6h) and treated with 10 nM insulin for the indicated times. Western blots of pSer473 AKT and pTyr1162/1163 INSR, n=4–6 independent experiments. (**D**) Human primary hepatocytes transduced with Ad-LacZ and Ad-ABCB10. Two days after transduction, hepatocytes were serum-starved (6h) and treated with 10 nM insulin for the indicated times. Western blots detecting pSer473 Akt and pTyr1162/1163 INSR in total lysates. n=3–5 independent experiments. Mean ± SEM, *p<0.05 One-way ANOVA.

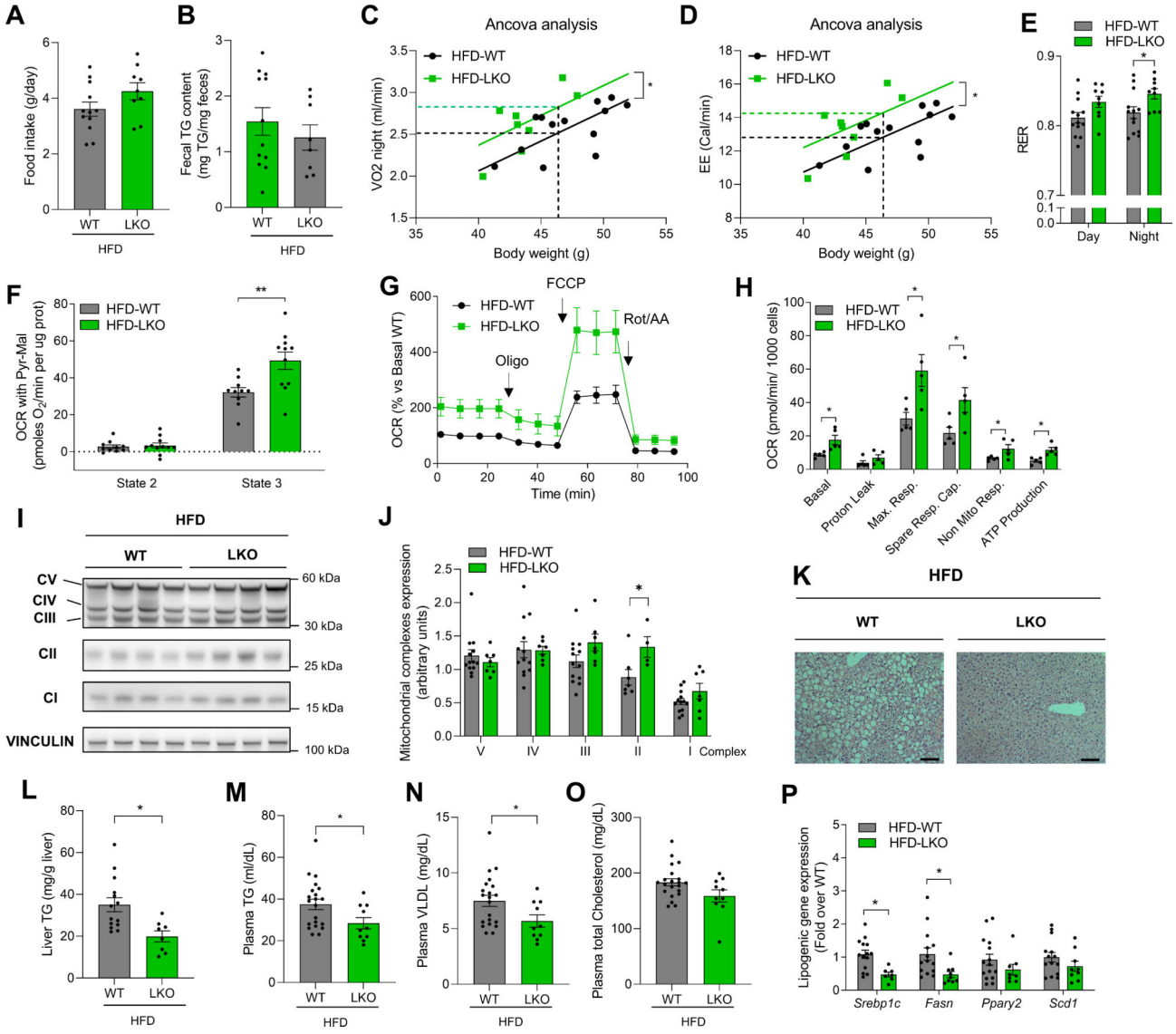

Fig. 5. Hepatic ABCB10 deletion increases mitochondrial energy expenditure and protects from hepatic steatosis and hyperlipidemia induced by high-fat diet.

(**A-O**) Measurements in WT and ABCB10-LKO male mice fed a high-fat diet (HFD) for 30–32 weeks. (**A**) Food intake of each individual mouse over a 48h period and (**B**) triglyceride (TG) content measured in feces collected in the metabolic cages (n=8–12 mice). (**C**) Co-variate analysis of VO_2 and (**D**) energy expenditure (EE) versus total body weight measured using CLAMS. Dashed lines represent the average body weight values modeled to determine VO_2 and EE in each group, *p<0.05 using ANCOVA, n=8–13 mice/group. (**E**) Respiratory exchange ratio (RER), *p<0.05, Student's t test; n=8–13 mice/group. (**F**) Oxygen consumption rates (OCR) from isolated liver mitochondria under state 2 (leak) and state 3 (maximal ATP synthesis) fueled by pyruvate (Pyr) and malate (Mal). n=10–12 mice/group, **p<0.01, Student's t-test. (**G**) OCR traces showing basal, ATP-synthesizing (oligomycin sensitive), and maximal respiration (induced by FCCP) and (**H**) their bar graph quantification measured in intact primary hepatocytes isolated from n=5 mice/group;

*p<0.05, Student's t-test. (**I-J**) Mitochondrial complex I to V subunits protein content in total liver lysates, with vinculin as loading control. n=7–13 mice/group. *p<0.05, Student's t-test WT vs LKO. (**K**) Hematoxylin & eosin staining of liver sections. Scale bar, 100 μm. (**L**) Liver triglyceride content in total liver lipid extracts. n=8–14 mice/ group; *p<0.05, Student's t-test. (**M**) Plasma triglyceride, (**N**) plasma very-low-density lipoprotein (VLDL) and (**O**) plasma total cholesterol concentration. n=10–21 mice per group. *p<0.05, Student's t-test. (**P**) Expression of lipogenic genes *Srebp1c*, *Fasn, Atgl, Pparγ2, Scd1* measured by qPCR of cDNA retrotranscribed from HFD fed-WT and LKO mouse livers. n=7–15 mice/ group. *p<0.05, Student's t-test. Results presented as mean ± SEM.

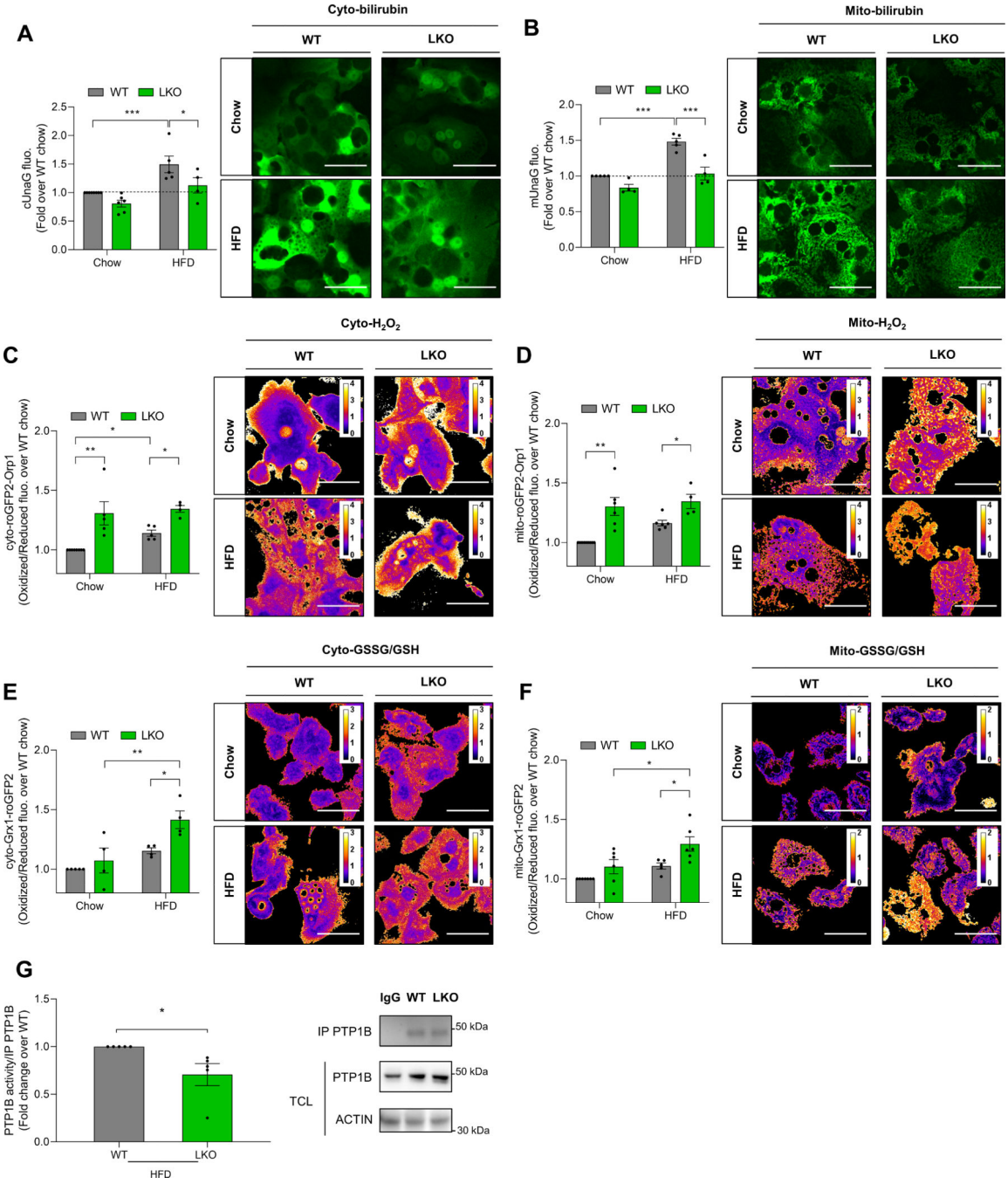

Fig. 6. Hepatic ABCB10 deletion increases mitochondrial H_2O_2 release and inactivates PTP1B, a phosphatase promoting hepatic insulin resistance and steatosis.

(**A-B**) Primary hepatocytes from lean (chow diet) and HFD-fed WT and ABCB10-LKO mice transduced with adenovirus encoding cytosolic UnaG (cUnaG), to measure cytosolic bilirubin content, or encoding mitochondrial matrix-targeted UnaG (mUnaG), to measure mitochondrial bilirubin. n=5–8 mice/group and independent experiments. Scale bar, 100 μm. Two-way ANOVA; *p<0.05, **p<0.01, ***p<0.001. (**C-F**) Primary hepatocytes isolated from WT and ABCB10-LKO mice fed a HFD for 30 weeks and transduced with adenovirus

encoding (**C**) Cyto-roGFP2-Orp1, measuring cytosolic H_2O_2 content, (**D**) Mito-roGFP2-Orp1, measuring mitochondrial matrix H_2O_2 content, (**E**) Cyto-Grx1-roGFP2 measuring cytosolic GSSG/GSH or (**F**) Mito-Grx1-roGFP2 measuring mitochondrial GSSG/GSH. The ratio of green fluorescence emitted by oxidized roGFP2 divided by reduced roGFP2 is proportional to H_2O_2 content (Orp1) and GSSG/GSH (Grx1) respectively. Scale bar, 100 μm. n=4–9 mice/group and independent isolations; *p<0.05, **p<0.01, Two-way ANOVA. (**G**) PTP1B activity measured in primary hepatocytes isolated from HFD-fed WT and ABCB10-LKO mice by immunoprecipitating PTP1B and measuring its phosphatase activity. n=5 mice/group and independent isolations; *p<0.05, Mann-Whitney U test. Results presented as mean ± SEM.

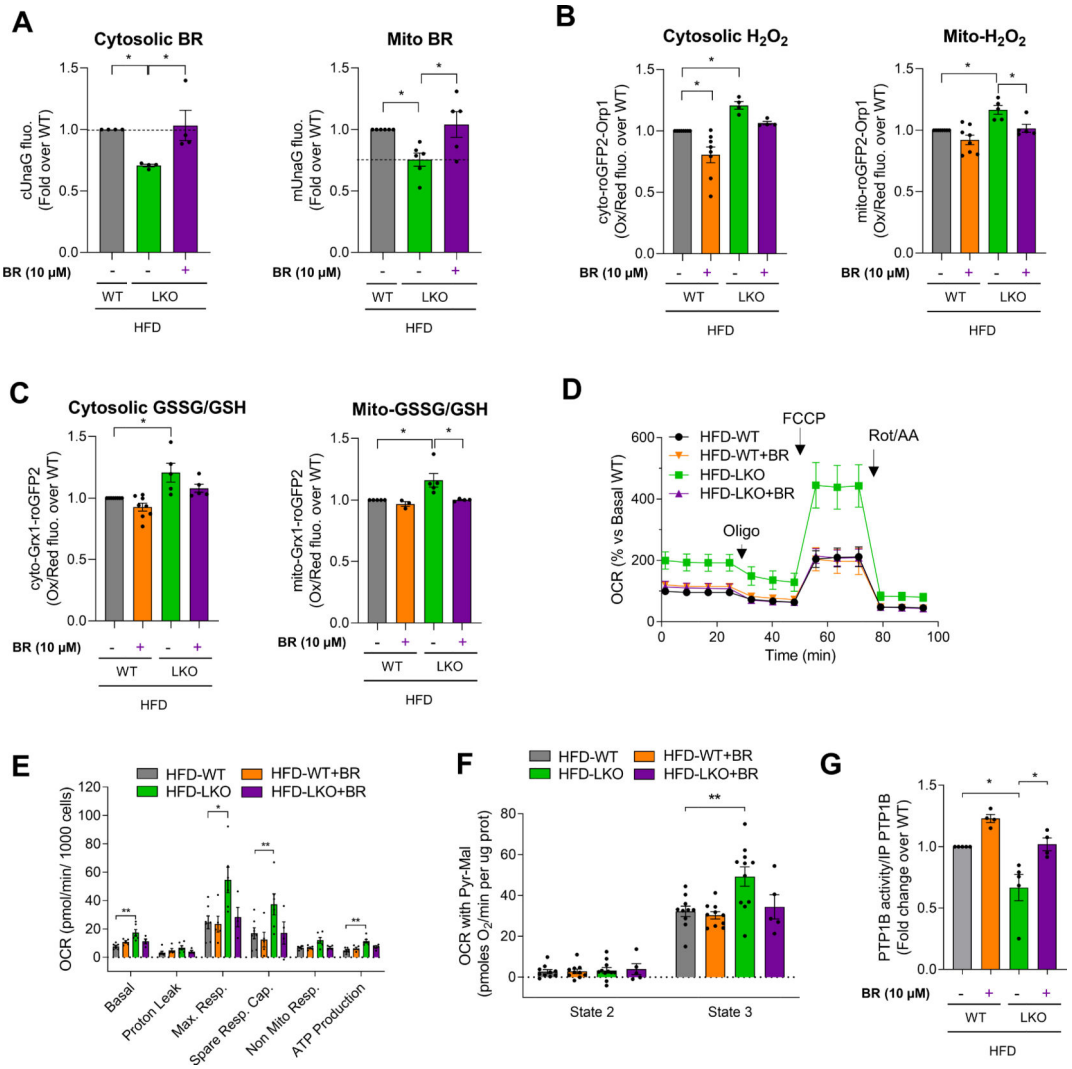

Fig. 7. Bilirubin supplementation reverses the redox benefits induced by hepatic ABCB10 deletion in diet-induced obese mice.

(**A**) Live imaging of cUnaG and mUnaG average fluorescence intensity to quantify cytosolic and mitochondrial bilirubin in hepatocytes isolated from HFD-fed ABCB10 LKO mice and then treated with vehicle (DMSO) and 10 μM bilirubin. Effects of the same bilirubin treatments on (**B**) cytosolic and mitochondrial matrix H_2O_2 content and (**C**) Grx1-roGFP2 and mito-Grx1-roGFP2 measuring cytosolic and mitochondrial GSSG/GSH. n = 3–8 mice/group. *p<0.05; Two-way ANOVA. (**D**) Respiration traces of primary hepatocytes treated with vehicle (DMSO) or 10 μM bilirubin (16h), isolated from HFD-fed WT and ABCB10 LKO mice. (**E**) Bar graph of respiration traces in (**D**) ± SEM. n=3–7 mice/group. Two-way ANOVA: *p<0.05 (**F**) Liver mitochondria isolated from HFD-fed WT and ABCB10 LKO mice respiring under state 2 (leak) and state 3 (maximal ATP synthesis) fueled by pyruvate (Pyr) and malate (Mal), with vehicle (DMSO) or 10 μM bilirubin (BR). n=5–11 mice/group. Two-way ANOVA; **p<0.01. (**G**) Phosphatase activity measured in immunoprecipitated PTP1B from primary hepatocytes treated with vehicle (DMSO) or 10 μM bilirubin (BR)

(16h) and isolated from HFD-fed WT and ABCB10 LKO mice. n= 4–5 mice/group. Two-way ANOVA, *p<0.05. Results presented as mean ± SEM.